cells) were cultured in 12-well culture plates overnight and then stimulated with 1 ng/mL of TGF-β1 for 6 h. Then culture supernatants were collected for analysis. Cytokine levels were expressed as the mean ± SEM for 3×10^5 cells.

Biochemical analysis of mouse sera

Serum ALT concentrations were measured with a Transaminase CII-test Wako Kit (Wako Pure Chemical Industries, Tokyo, Japan).

Mouse HSC oligo-DNA microarray analysis

To investigate the gene expression differences between Tg-HSCs and WT-HSCs, we performed DNA microarray analysis of mice HSCs (Whole Mouse Genome Microarray Kit, 4 × 44 K; Agilent Technology, Tokyo, Japan). Total RNA was extracted from HSCs isolated from WT and Tg mice with a QIAshredder and an RNeasy Mini Kit according to the instructions provided by the manufacturer (Qiagen). Total RNA (200 ng) was labeled with Cy-3 or Cy-5 using a Quick Amp Labeling Kit, two-color. Fluorescently labeled targets were hybridized with a Gene Expression Hybridization Kit. The hybridization process was performed according to the manufacturer's instructions, and hybridized microarrays were scanned using an Agilent Microarray Scanner. Agilent's Feature Extraction software was used for the image analysis and data extraction processes.

Statistical analysis

The results are presented as the mean ± SEM. Analysis of variance for the groups was performed by means of the Kruskal–Wallis test, followed by the Scheffe test for multiple comparisons to allow pairwise testing for significant differences between groups. Statistical significance was defined as $P < 0.05$.

Supplementary Data

Supplementary data for this article is available online at http://glycob.oxfordjournals.org/.

Funding

This study was supported by a grant from the Global COE program of Osaka University funded by the Ministry of Education, Culture, Sports, Science, and Technology of Japan, a Grant-in-Aid for Scientific Research (A), No. 21249038, from the Japan Society for the Promotion of Science, and a Grant-in-Aid for Scientific Research (C), No. 20590777, from the Japan Society for the Promotion of Science.

Conflict of interest

None declared.

Abbreviations

ALT, alanine aminotransferase; CLD, chronic liver disease; COX2, cyclooxygenase-2; DMEM, Dulbecco's modified Eagle's medium; EGFR, epidermal growth factor receptor; EMT, epithelial–mesenchymal transition; GAPDH, glyceraldehyde 3-phosphate dehydrogenase; GnT-V, *N*-acetylglucosaminyltransferase V; HEPES, 4-(2-hydroxyethyl)-1-piperazineethanesulfonic acid; HFHC, high fat and high cholesterol; HSC, hepatic stellate cell; IFN-γ, interferon-γ; IL, interleukin; MCP-1, monocyte chemoattractant protein-1; NAFLD, non-alcoholic fatty liver disease; NASH, non-alcoholic steatohepatitis; NC, normal chow; NOS2, nitric oxide synthase 2; PDGF, platelet-derived growth factor; PGE2, prostaglandin E2; RT–PCR, reverse transcription–polymerase chain reaction; SDS, sodium dodecyl sulfate; TCR, T-cell antigen receptor; Tg, transgenic; TG, triglyceride; TGF, transforming growth factor; Tg-HSC, Tg mouse-derived HSC; TNF-α, tumor necrosis factor-α; WT, wild type; WT-HSC, WT mouse-derived HSC.

References

Bugianesi E, Leone N, Vanni E, Marchesini G, Brunello F, Carucci P, Musso A, De Paolis P, Capussotti L, Salizzoni M, et al. 2002. Expanding the natural history of nonalcoholic steatohepatitis: From cryptogenic cirrhosis to hepatocellular carcinoma. *Gastroenterology*. 123:134–140.

Demetriou M, Granovsky M, Quaggin S, Dennis JW. 2001. Negative regulation of T-cell activation and autoimmunity by Mgat5 N-glycosylation. *Nature*. 409:733–739.

Deushi M, Nomura M, Kawakami A, Haraguchi M, Ito M, Okazaki M, Ishii H, Yoshida M. 2007. Ezetimibe improves liver steatosis and insulin resistance in obese rat model of metabolic syndrome. *FEBS Lett.* 581:5664–5670.

Ford ES, Giles WH, Dietz WH. 2002. Prevalence of the metabolic syndrome among US adults: Findings from the third National Health and Nutrition Examination Survey. *JAMA*. 287:356–359.

Gao Y, Song LX, Jiang MN, Ge GY, Jia YJ. 2008. Effects of traditional Chinese medicine on endotoxin and its receptors in rats with non-alcoholic steatohepatitis. *Inflammation*. 31:121–132.

Granovsky M, Fata J, Pawling J, Muller WJ, Khokha R, Dennis JW. 2000. Suppression of tumor growth and metastasis in Mgat5-deficient mice. *Nat Med*. 6:306–312.

Haukeland JW, Damas JK, Konopski Z, Loberg EM, Haaland T, Goverud I, Torjesen PA, Birkeland K, Bjoro K, Aukrust P. 2006. Systemic inflammation in nonalcoholic fatty liver disease is characterized by elevated levels of CCL2. *J Hepatol*. 44:1167–1174.

Hui AY, Dannenberg AJ, Sung JJ, Subbaramaiah K, Du B, Olinga P, Friedman SL. 2004. Prostaglandin E2 inhibits transforming growth factor beta 1-mediated induction of collagen alpha 1(I) in hepatic stellate cells. *J Hepatol*. 41:251–258.

Hyogo H, Tazuma S, Arihiro K, Iwamoto K, Nabeshima Y, Inoue M, Ishitobi T, Nonaka M, Chayama K. 2008. Efficacy of atorvastatin for the treatment of nonalcoholic steatohepatitis with dyslipidemia. *Metabolism*. 57:1711–1718.

Kristensen DB, Kawada N, Imamura K, Miyamoto Y, Tateno C, Seki S, Kuroki T, Yoshizato K. 2000. Proteome analysis of rat hepatic stellate cells. *Hepatology*. 32:268–277.

Lau KS, Dennis JW. 2008. *N*-Glycans in cancer progression. *Glycobiology*. 18:750–760.

Lee RT, Lee YC. 2000. Affinity enhancement by multivalent lectin-carbohydrate interaction. *Glycoconj J*. 17:543–551.

Li MO, Flavell RA. 2008. TGF-beta: A master of all T cell trades. *Cell*. 134:392–404.

Massague J. 2000. How cells read TGF-beta signals. *Nat Rev Mol Cell Biol*. 1:169–178.

Matsuzawa N, Takamura T, Kurita S, Misu H, Ota T, Ando H, Yokoyama M, Honda M, Zen Y, Nakanuma Y, et al. 2007. Lipid-induced oxidative stress causes steatohepatitis in mice fed an atherogenic diet. *Hepatology*. 46:1392–1403.

Miyoshi E, Ihara Y, Nishikawa A, Saito H, Uozumi N, Hayashi N, Fusamoto H, Kamada T, Taniguchi N. 1995. Gene expression of N-acetylglucosaminyltransferases III and V: A possible implication for liver regeneration. *Hepatology.* 22:1847–1855.

Miyoshi E, Nishikawa A, Ihara Y, Gu J, Sugiyama T, Hayashi N, Fusamoto H, Kamada T, Taniguchi N. 1993. N-acetylglucosaminyltransferase III and V messenger RNA levels in LEC rats during hepatocarcinogenesis. *Cancer Res.* 53:3899–3902.

Morgan R, Gao G, Pawling J, Dennis JW, Demetriou M, Li B. 2004. N-acetylglucosaminyltransferase V (Mgat5)-mediated N-glycosylation negatively regulates Th1 cytokine production by T cells. *J Immunol.* 173:7200–7208.

Ohtsubo K, Marth JD. 2006. Glycosylation in cellular mechanisms of health and disease. *Cell.* 126:855–867.

Park HJ, Partridge E, Cheung P, Pawling J, Donovan R, Wrana JL, Dennis JW. 2006. Chemical enhancers of cytokine signaling that suppress microfilament turnover and tumor cell growth. *Cancer Res.* 66: 3558–3566.

Partridge EA, Le Roy C, Di Guglielmo GM, Pawling J, Cheung P, Granovsky M, Nabi IR, Wrana JL, Dennis JW. 2004. Regulation of cytokine receptors by Golgi N-glycan processing and endocytosis. *Science.* 306:120–124.

Taniguchi N, Ihara S, Saito T, Miyoshi E, Ikeda Y, Honke K. 2001. Implication of GnT-V in cancer metastasis: A glycomic approach for identification of a target protein and its unique function as an angiogenic cofactor. *Glycoconj J.* 18:859–865.

Taniguchi N, Miyoshi E, Ko JH, Ikeda Y, Ihara Y. 1999. Implication of N-acetylglucosaminyltransferases III and V in cancer: Gene regulation and signaling mechanism. *Biochim Biophys Acta.* 1455:287–300.

Terao M, Ishikawa A, Nakahara S, Kimura A, Kato A, Moriwaki K, Kamada Y, Murota H, Taniguchi N, Katayama I, et al. 2011. Enhanced epithelial-mesenchymal transition-like phenotype in N-acetylglucosaminyltransferase V transgenic mouse skin promotes wound healing. *J Biol Cem.* 286: 28303–28311.

Yasutake K, Nakamuta M, Shima Y, Ohyama A, Masuda K, Haruta N, Fujino T, Aoyagi Y, Fukuizumi K, Yoshimoto T, et al. 2009. Nutritional investigation of non-obese patients with non-alcoholic fatty liver disease: The significance of dietary cholesterol. *Scand J Gastroenterol.* 44:471–477.

Yoshimura A, Wakabayashi Y, Mori T. 2010. Cellular and molecular basis for the regulation of inflammation by TGF-beta. *J Biochem.* 147:781–792.

Zhao Y, Sato Y, Isaji T, Fukuda T, Matsumoto A, Miyoshi E, Gu J, Taniguchi N. 2008. Branched N-glycans regulate the biological functions of integrins and cadherins. *FEBS J.* 275:1939–1948.

Altered Oligosaccharide Structures Reduce Colitis Induction in Mice Defective in β-1,4-Galactosyltransferase

SHINICHIRO SHINZAKI,[*,‡] HIDEKI IIJIMA,[*] HIRONOBU FUJII,[‡] ERI KUROKI,[‡] NORIKA TATSUNAKA,[‡] TAKAHIRO INOUE,[*] SACHIKO NAKAJIMA,[*] SATOSHI EGAWA,[*] TATSUYA KANTO,[*,§] MASAHIKO TSUJII,[*] EIICHI MORII,[‖] SHUNSAKU TAKEISHI,[¶] MASAHIDE ASANO,[#] TETSUO TAKEHARA,[*] NORIO HAYASHI,[*] and EIJI MIYOSHI[‡]

Departments of Gastroenterology and Hepatology, ‡Molecular Biochemistry and Clinical Investigation, §Dendritic Cell Biology and Clinical Application, and ‖Pathology, Osaka University Graduate School of Medicine, Osaka; ¶GP BioScience Ltd, Yokohama; and the #Division of Transgenic Animal Science, Kanazawa University Advanced Science Research Center, Kanazawa, Japan

BACKGROUND & AIMS: Oligosaccharide modifications induce various functional changes in immune cells. The galactose-deficient fraction of fucosylated IgG oligosaccharides is increased, whereas that of β-1,4-galactosyltransferase I (B4GalTI) is reduced, in patients with Crohn's disease. We investigated the role of oligosaccharide modification in the pathophysiology of colitis using *B4galt1*-deficient mice. **METHODS:** Colitis severity was compared between *B4galt1*$^{+/-}$ and *B4galt1*$^{+/+}$ mice. B cells isolated from *B4galt1*$^{+/-}$ and *B4galt1*$^{+/+}$ mice were adoptively transferred to recombination activating gene 2$^{-/-}$ mice, in which colitis was induced by administration of CD4^{+}CD62L^{+} T cells. Cell-surface glycan profiles were determined by lectin microarray analysis. Cytokine production was determined in a coculture of various types of cells isolated from either *B4galt1*$^{+/-}$ or *B4galt1*$^{+/+}$ mice. **RESULTS:** Colitis induction by dextran sodium sulfate or trinitrobenzene sulfonic acid was significantly reduced in *B4galt1*$^{+/-}$ mice, which had galactose deficiency in IgG oligosaccharides (similar to patients with Crohn's disease) compared with *B4galt1*$^{+/+}$ mice. Amelioration of colitis was associated with increased production of interleukin-10 by macrophages in *B4galt1*$^{+/-}$ mice. Colitis induction in recombination activating gene 2$^{-/-}$ mice by administration of CD4^{+}CD62L^{+} T cells was reduced by cotransfer of B cells isolated from *B4galt1*$^{+/-}$, but not from *B4galt1*$^{+/+}$ mice. Lectin microarray analysis revealed increased expression of polylactosamines on *B4galt1*$^{+/-}$ B cells and macrophages, compared with *B4galt1*$^{+/+}$ cells. The production of interleukin-10 from macrophages was induced via their direct interaction with *B4galt1*$^{+/-}$ B cells. **CONCLUSIONS: Altered oligosaccharide structures on immune cells modulate mucosal inflammation. Oligosaccharides in immune cells might be a therapeutic target for inflammatory bowel diseases.**

Keywords: IBD; Mouse Model; Immune Regulation; CD.

BASIC AND TRANSLATIONAL AT

Inflammatory bowel disease (IBD), including Crohn's disease (CD) and ulcerative colitis, is characterized as a chronic relapsing and remitting process in the digestive tract. Although the precise etiology of IBD remains unknown, both genetic susceptibility and dysregulation of mucosal immune responses against enteric host flora have pivotal roles in its pathogenesis.[1] We recently demonstrated that oligosaccharide structures in serum IgG are dynamically changed in patients with IBD compared with healthy subjects.[2] IgG carries *N*-linked oligosaccharides at the Cγ2 domain of the Fc fragment at asparagine 297.[3,4] The proportion of the agalactosyl fraction in the fucosylated oligosaccharides of human IgG is significantly higher in patients with CD than in patients with ulcerative colitis or in healthy volunteers.[2] In addition, agalactosyl IgG levels correlate with disease activity and the clinical course of CD.[2] These findings suggest that changes in the IgG oligosaccharide structure relate to the pathogenesis of CD. β-1,4-galactosyltransferase I (B4GalTI) conjugates galactose to the outer arm of *N*-acetylglucosamine in *N*-linked oligosaccharides of IgG and B4GalTI levels are associated with extension of the terminal galactose in IgG.[5] In fact, B4GalTI activity and messenger RNA expression in B cells or plasma cells are lower in CD than in ulcerative colitis or disease controls.[2] The roles of oligosaccharide alterations in CD, however, have not yet been investigated.

Recent reports demonstrate that B cells and immunoglobulins have protective roles in IBD. Mizoguchi et al reported that B cells in mesenteric lymph nodes (MLN) containing the regulatory B-cell subset protects against colitis in murine colitis models.[6] Intravenous immunoglobulin therapy is also effective for the treatment of human IBD.[7] Although immunoglobulins and B cells have protective roles in IBD, it is not known whether oligosaccharide alterations via B4GalTI deficiency affect immune function in CD.

In the present study, we explored the pathophysiologic role of agalactosyl oligosaccharide alterations in IBD using murine colitis models. We found that *B4galt1*$^{+/-}$ mice, which exhibit decreased B4GalTI activity, were protected against murine colitis models compared with wild-type mice with up-regulation of interleukin (IL)-10 production

Abbreviations used in this paper: B4GalTI, β-1,4-galactosyltransferase I; CD, Crohn's disease; DSA, *Datura stramonium* agglutinin; DSS, dextran sodium sulfate; IBD, inflammatory bowel disease; IFN, interferon; IL, interleukin; LP, lamina propria; LPS, lipopolysaccharides; MLN, mesenteric lymph nodes; PE, phycoerythrin; *Rag*, recombination activating gene; SP, spleen; TNBS, trinitrobenzene sulfonic acid.

0016-5085/$36.00
doi:10.1053/j.gastro.2012.02.008

from macrophages. The mechanisms for the enhanced production of IL-10 due to the alteration of oligosaccharides were further evaluated.

Materials and Methods

Mice

B4galt1$^{+/-}$ mice (C57BL/6 background) were generated as described previously.[8] *Il-10*$^{-/-}$ mice (C57BL/6 background) were purchased from the Jackson Laboratory (Bar Harbor, ME). C57BL/6 mice and recombination activating gene *(Rag) 2*$^{-/-}$ mice were purchased from Japan Clea (Tokyo, Japan) and Taconic Inc. (Hudson, NY), respectively. All mice were kept under specific pathogen-free conditions in an environmentally controlled clean room at the Institute of Experimental Animal Sciences, Osaka University Graduate School of Medicine. The Institutional Committee on Animal Research approved the experiments.

Induction of Colitis

To generate dextran sodium sulfate (DSS)–induced colitis, mice were provided with 3% DSS (molecular weight 35,000–50,000 Da; MP Biomedicals, Solon, OH) in the drinking water ad libitum for 7 days. After administration of normal water for the following 3 days, the mice were killed on day 10. Trinitrobenzene sulfonic acid (TNBS)–induced colitis was generated as described previously.[9] To generate colitis by adoptive transfer, CD4$^+$CD62L$^+$ naïve T cells were transferred to immunodeficient *Rag2*$^{-/-}$ mice as described previously.[10] Briefly, splenic CD4$^+$CD62L$^+$ cells isolated from female C57BL/6 mice using a mouse CD4 naïve T-cell column kit (R&D Systems, Minneapolis, MN) were intraperitoneally injected into *Rag2*$^{-/-}$ mice (5×10^5 cells/mouse). Mice were killed at 10 weeks after transfer. In some experiments, CD19$^+$ B cells were isolated from the MLN of *B4galt1*$^{+/-}$ or *B4galt1*$^{+/+}$ mice with CD19 magnetic beads (Miltenyi Biotech, Bergisch Gladbach, Germany), and 5×10^5 cells were intraperitoneally injected into *Rag2*$^{-/-}$ mice.

Serum IgG Oligosaccharide Analysis

IgG purification from the sera of mice and subsequent IgG oligosaccharide analysis were performed as described previously.[2] Briefly, serum IgG was purified using protein G sepharose and *N*-linked oligosaccharides were released from serum IgG, labeled with 2-aminopyridine, and analyzed on a reversed phase high-performance liquid chromatography system (Waters Corp., Milford, MA).

Histologic Analysis

Formalin-fixed tissue samples were paraffin-embedded and proximal/distal colon sections were analyzed by H&E staining. Histologic scores were determined using individual scores for DSS colitis,[11] TNBS colitis,[9] IL-10–deficient colitis,[12] and CD4$^+$CD62L$^+$ adoptive-transferred colitis.[13] Histology was examined by a well-trained pathologist (E.M.) in a blinded manner. Immunohistochemistry was performed using anti-mouse B220 antibody (BD Biosciences, San Jose, CA) as described previously.[14]

Cytokine Analysis and Myeloperoxidase Activity

Mononuclear cells from the spleen (SP), MLN, and colonic lamina propria (LP) were collected as described previously.[15] CD4$^+$ T cells, B cells, and macrophages were separated with CD4, CD19, and CD11b magnetic beads, respectively (Miltenyi Biotech). Cells (10^6 cells) were cultured in flat bottom 96-well culture plates for 48 hours in RPMI 1640 (Sigma-Aldrich, St Louis, MO) with 10% fetal bovine serum and antibiotics/antimycotics in the presence of hamster anti-mouse CD3 and hamster anti-mouse CD28 antibodies (5 μg/mL; BD Biosciences) for the culture of whole mononuclear cells and T cells, or in the presence of 1 μg/mL lipopolysaccharides (LPS) from *Escherichia coli* (O111:B4; Sigma-Aldrich) for B cells and macrophages. In coculture assay, 2×10^5 macrophages were cocultured with the same number of B cells in 96-well plates. In separate experiments, macrophages and B cells were cultured while separated by Transwell culture inserts (0.4-μm pore-size; BD Falcon, Franklin Lakes, NJ). In some experiments, macrophages and B cells were preincubated with lactose or sucrose (Nakalai Tesque Inc., Kyoto, Japan).[16] Macrophages were stimulated with recombinant mouse galectin-1, 3, or 4 (R&D Systems) or vehicle in the presence of LPS. Culture supernatant was collected and cytokine productions of interferon (IFN)-γ, IL-10, IL-17, IL-4, and transforming growth factor–β were determined by enzyme-linked immunosorbent assay (eBioscience, San Diego, CA) according to manufacturer's instructions. Cytokine levels are expressed as the mean ± standard error of mean of 10^6 cells. Myeloperoxidase activity of the colon was investigated using Myeloperoxidase Chlorination Assay Kit (Cayman Chemical Co, Ann Arbor, MI) according to manufacturers' instructions.

Lectin Microarray

The total pattern of oligosaccharide structures in serum IgG was investigated using an evanescent-field fluorescence-assisted lectin micro array as described previously.[17] Briefly, 45 lectins were immobilized on a glass slide in triplicate, and cellular protein was applied to the array. A fluorescence image of the array was acquired using an evanescent-field fluorescence scanner, GTMASScan III (Nippon Laser & Electronics Lab, Nagoya, Japan).

Flow Cytometric Analysis

Cells were stained with fluorescein isothiocyanate–labeled *Datura stramonium* agglutinin (DSA) or *Ricinus communis* agglutinin 120 (J-Oil Mills, Inc. Tokyo, Japan). Pacific Blue–labeled anti-CD4, phycoerythrin (PE)-labeled anti-CD19, anti-CD25-PE (BD Biosciences), anti-CD11b–fluorescein isothiocyanate, anti-CD11c-PE, and anti-F4/80-PE (eBioscience) were also used. Intracellular IL-10 or Foxp3 was stained using allophycocyanin-labeled anti-IL-10 or Alexa Fluor 488–labeled anti-Foxp3 antibody with Cytofix/Cytoperm (BD Biosciences) according to manufacturer's instructions. These samples were subjected to flow cytometric analysis using a FACS Canto II (BD Biosciences). Data were analyzed using FlowJo software (Tree-Star Inc., Ashland, OR).

Statistical Analysis

Results are expressed as mean ± standard error of mean. Groups of data were compared by the Mann-Whitney *U* test. Differences were considered statistically significant when $P < .05$.

Results

Serum IgG of B4galt1$^{+/-}$ *Mice Has an Agalactosyl Pattern Similar to That of Patients With CD*

B4GalTI is involved in the biosynthesis of galactose-containing oligosaccharides and is a major galactosyltransferase responsible for selectin ligand biosynthesis among the β4galactosyltransferase gene family.[18] We first analyzed the IgG oligosaccharide structures of *B4galt1*$^{-/-}$ mice by reverse-phase high-performance liquid chromatography. The peak of the agalactosyl fraction in the fucosylated oligosaccharides (G0F) was smaller than that of the full galactosyl fraction (G2F) in *B4galt1*$^{+/+}$ mice. In marked contrast, the mono-galactosyl (G1F) and G2F oligosaccharide peaks were almost completely absent in *B4galt1*$^{-/-}$ mice (Figure 1*A*). This finding suggests that B4GalTI exclusively regulates the attachment of galactose to IgG oligosaccharides. A previous report indicated that B4GalTI enzyme activity in *B4galt1*$^{+/-}$ mice is almost half that in *B4galt1*$^{+/+}$ mice.[8] In fact, the G2F peak in *B4galt1*$^{+/-}$ mice was much smaller than that in *B4galt1*$^{+/+}$ mice, and the G0F peak in *B4galt1*$^{+/-}$ mice was larger than that of G2F in *B4galt1*$^{+/-}$ mice (Figure 1*A*). *B4galt1*$^{-/-}$ mice exhibit poor survival and, if born alive, have severely retarded growth.[8] Therefore, *B4galt1*$^{-/-}$ mice cannot be used for colitis experiments. We realized, however, that the IgG oligosaccharide structures of *B4galt1*$^{+/-}$ mice and *B4galt1*$^{+/+}$ mice resemble those of the patients with CD and healthy subjects, respectively.[2] We therefore used *B4galt1*$^{+/-}$ mice to investigate the role of agalactosyl oligosaccharides in IBD.

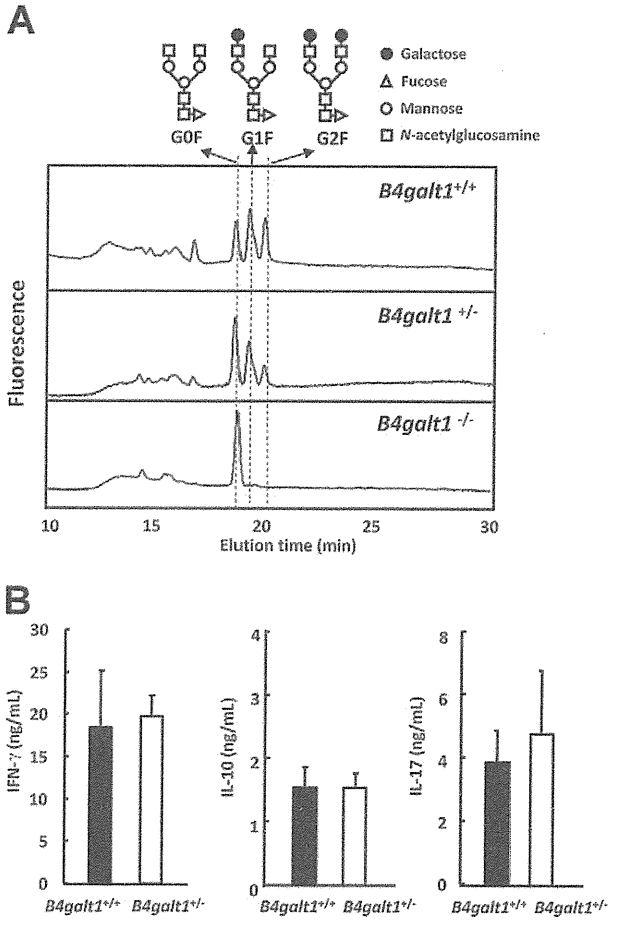

Figure 1. Biochemical and immunologic characteristics of *B4galt1*-deficient mice before the induction of colitis. (*A*) Oligosaccharide structures attached to serum IgG in *B4galt1*$^{+/+}$, *B4galt1*$^{+/-}$, and *B4galt1*$^{-/-}$ mice. Structures of *N*-linked oligosaccharides were analyzed by reversed-phase high-performance liquid chromatography. (*B*) Cytokine production of *B4galt1*$^{+/+}$ and *B4galt1*$^{+/-}$ mice. Splenic mononuclear cells were cultured with anti-CD3 and anti-CD28 monoclonal antibodies for 48 hours and cytokine production of IFN-γ, IL-10, and IL-17 in the culture supernatants was determined by enzyme-linked immunosorbent assay. Data are shown as the mean ± standard error of mean of 4 independent experiments.

Under specific-pathogen–free conditions, there were no differences in the proportions of the T and B cells and macrophage populations in the SP, MLN, and colonic LP between *B4galt1*$^{+/-}$ and *B4galt1*$^{+/+}$ mice (data not shown). In addition, the cytokine production levels of IFN-γ, IL-17, and IL-10 in the SP were not significantly different between *B4galt1*$^{+/-}$ and *B4galt1*$^{+/+}$ mice (Figure 1*B*). Cytokine production in MLN or colonic LP was not significantly different between *B4galt1*$^{+/-}$ and *B4galt1*$^{+/+}$ mice, and *B4galt1*$^{+/-}$ mice showed no apparent signs of colitis (data not shown). We confirmed that the baseline immunologic status did not differ between *B4galt1*$^{+/-}$ and *B4galt1*$^{+/+}$ mice.

DSS-Induced Colitis Is Ameliorated in B4galt1$^{+/-}$ *Mice Compared to* B4galt1$^{+/+}$ *Mice*

We next investigated the severity of DSS-induced colitis in *B4galt1*$^{+/-}$ and *B4galt1*$^{+/+}$ mice. *B4galt1*$^{+/-}$ mice that treated with DSS had significantly decreased body weight loss (Figure 2*A*). In addition, the colons of *B4galt1*$^{+/-}$ mice that received DSS exhibited significantly less shortening and thickening than those of *B4galt1*$^{+/+}$ mice (Figure 2*B*, *C*). Consistent with these macroscopic changes, *B4galt1*$^{+/-}$ mice had less severe histologic features of colitis than *B4galt1*$^{+/+}$ mice (Figure 2*D*). In addition, *B4galt1*$^{+/-}$ mice had significantly lower colitis scores than *B4galt1*$^{+/+}$ mice (Figure 2*E*). The oligosaccharide structures of IgG, as determined by reversed-phase high-performance liquid chromatography were unchanged before and after the induction of colitis in *B4galt1*$^{+/-}$ and *B4galt1*$^{+/+}$ mice (data not shown).

Increased Production of IL-10 in Macrophages of B4galt1$^{+/-}$ *Mice*

To determine if the amelioration of colitis in *B4galt1*$^{+/-}$ mice is associated with changes in cytokine production, we examined the cytokine production of mononuclear cells isolated from the SP, MLN, and LP of *B4galt1*$^{+/+}$ and *B4galt1*$^{+/-}$ mice with DSS colitis. Although the differences in IFN-γ and IL-17 production between the 2 groups were not significantly different (Figure 3*A*, *B*), IL-10 production in the SP, MLN, and LP from

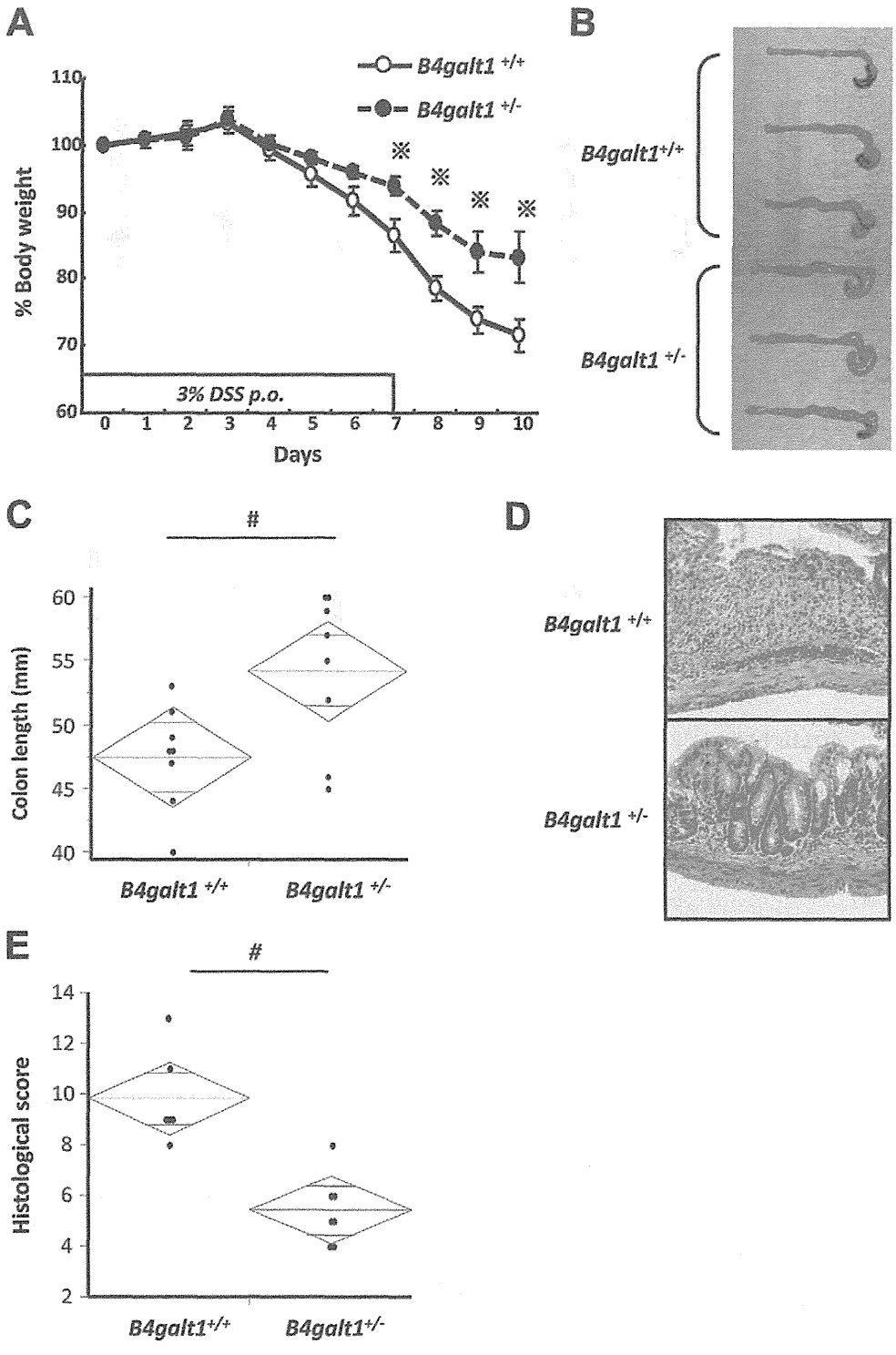

Figure 2. Amelioration of DSS-induced colitis in *B4galt1*$^{+/-}$ mice. (*A*) Body weight of *B4galt1*$^{+/+}$ and *B4galt1*$^{+/-}$ mice subjected to DSS-induced colitis. ※Body weight was significantly greater in *B4galt1*$^{+/-}$ mice than *B4galt1*$^{+/+}$ mice. (*B*) Macroscopic pictures of the colons from *B4galt1*$^{+/+}$ and *B4galt1*$^{+/-}$ mice. (*C*) Colon length of *B4galt1*$^{+/+}$ and *B4galt1*$^{+/-}$ mice. (*D*) Representative micrographs of H&E-stained colon. (*E*) Histologic scores of DSS colitis in *B4galt1*$^{+/+}$ and *B4galt1*$^{+/-}$ mice. Data are shown as mean ± standard error of mean of 8 mice per group. #$P < .05$.

B4galt1$^{+/-}$ mice was significantly higher than that in *B4galt1*$^{+/+}$ mice (Figure 3*C*). We then purified CD4$^+$ T cells, CD19$^+$ B cells, and CD11b$^+$ macrophages/dendritic cells from the SP of *B4galt1*$^{+/-}$ and *B4galt1*$^{+/+}$ mice to investigate the source of the IL-10 production. IL-10 production by CD11b$^+$ cells isolated from *B4galt1*$^{+/-}$ mice was significantly higher than that from *B4galt1*$^{+/+}$ mice, while there was no difference in IL-10 production from CD4$^+$ T cells or from CD19$^+$ B cells obtained from *B4galt1*$^{+/-}$ and *B4galt1*$^{+/+}$ mice (Figure 3*D*). The production of IL-4 and transforming growth factor−β in the colon between the 2 groups was not significantly different (Supplementary Figure 1*A*, *B*). When CD11b$^+$ cells in colonic LP were intracellularly co-stained with anti−IL-10 antibody, CD11b$^+$F4/80$^+$ macrophages of *B4galt1*$^{+/-}$ mice produced more IL-10 than those of *B4galt1*$^{+/+}$ mac-

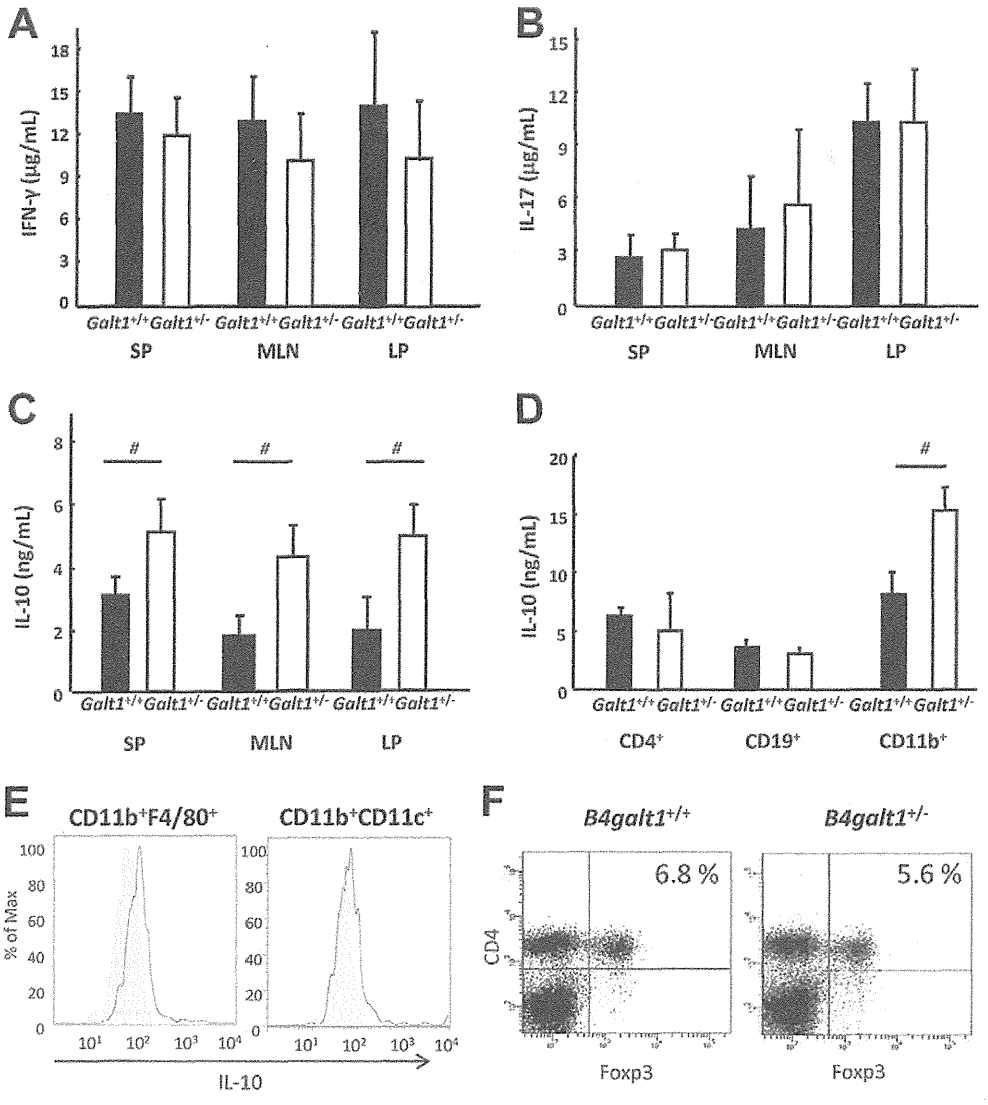

Figure 3. Cytokine production in *B4galt1*$^{+/+}$ and *B4galt1*$^{+/-}$ mice subjected to DSS-induced colitis. Mononuclear cells of the spleen (SP), mesenteric lymph nodes (MLN), and colonic LP isolated from *B4galt1*$^{+/+}$ (*Galt1*$^{+/+}$) and *B4galt1*$^{+/-}$ (*Galt1*$^{+/-}$) mice administered DSS were cultured in vitro for 48 hours and the levels of IFN-γ (*A*), IL-17 (*B*), and IL-10 (*C*) were measured by enzyme-linked immunosorbent assay. (*D*) IL-10 production of purified CD4$^+$ T cells, CD19$^+$ B cells, and CD11b$^+$ cells of DSS-induced splenocytes of *B4galt1*$^{+/+}$ and *B4galt1*$^{+/-}$ mice. Data are shown as mean ± standard error of mean of 4 independent experiments. $^{\#}P < .05$. (*E*) Flow cytometric analysis of IL-10 production in CD11b$^+$F4/80$^+$ macrophages and CD11b$^+$CD11c$^+$ dendritic cells in the colonic LP. *Solid line*, *B4galt1*$^{+/-}$; *shaded area*, *B4galt1*$^{+/+}$ mice. (*F*) Flow cytometric analysis of CD4$^+$Foxp3$^+$ regulatory T cells in *B4galt1*$^{+/+}$ and *B4galt1*$^{+/-}$ mice. Representative pictures are shown.

rophages, whereas there was no difference in IL-10 production in the CD11b$^+$CD11c$^+$ dendritic cell population (Figure 3*E*). In addition, the proportion of CD4$^+$Foxp3$^+$ and CD4$^+$CD25$^+$ regulatory T cells between the 2 groups was not significantly different (Figure 3*F*, Supplementary Figure 1*C*).

TNBS-Induced Colitis Is Ameliorated in B4galt1$^{+/-}$ *Mice Compared to* B4galt1$^{+/+}$ *Mice*

To eliminate the possibility that alterations in the absorption of the sugar portion of DSS in *B4galt1*$^{+/-}$ mice accounted for the observed difference in colitis severity, we also analyzed the severity of TNBS-induced colitis. Similarly to DSS-induced colitis, *B4galt1*$^{+/-}$ mice tended to show less severe body-weight loss and shortening of the colon than *B4galt1*$^{+/+}$ mice (Figures 4*A, B*, Supplementary Figure 3*A*). In addition, *B4galt1*$^{+/-}$ mice had significantly less severe histologic feature and myeloperoxidase activity of TNBS colitis than *B4galt1*$^{+/+}$ mice (Figures 4*C*–*E*). Although the production of IFN-γ and IL-17 between the 2 groups was not significantly different (Supplementary Figure 3*B, C*), IL-10 production in colonic LP isolated from *B4galt1*$^{+/-}$ mice were significantly higher than that from *B4galt1*$^{+/+}$ mice (Figure 4*E*).

Amelioration of Colitis in B4galt1$^{+/-}$ *Mice Is Lost in the Absence of IL-10*

Amelioration of colitis in *B4galt1*$^{+/-}$ mice was associated with an increased production of IL-10. We next sought to determine whether IL-10 has a critical role for the protection against colitis in *B4galt1*$^{+/-}$ mice. *Il-10*$^{-/-}$ mice, which develop spontaneous and chronic colitis at the age of 7 to 11 weeks,[19] were crossed with *B4galt1*$^{+/-}$ mice to generate *Il-10*$^{-/-}$*B4galt1*$^{+/-}$ mice. Body weight and macroscopic and histologic findings were not different between *Il-10*$^{-/-}$*B4galt1*$^{+/-}$ and *Il-10*$^{-/-}$*B4galt1*$^{+/+}$ mice (Figure 5*A*–*E*). In addition, IFN-γ and IL-17 production in the SP, MLN, and LP were not significantly different between *Il-10*$^{-/-}$*B4galt1*$^{+/-}$ and *Il-10*$^{-/-}$*B4galt1*$^{+/+}$ mice (data not shown). Thus, the amelioration of colitis in *B4galt1*$^{+/-}$ mice was lost in the absence of IL-10. These

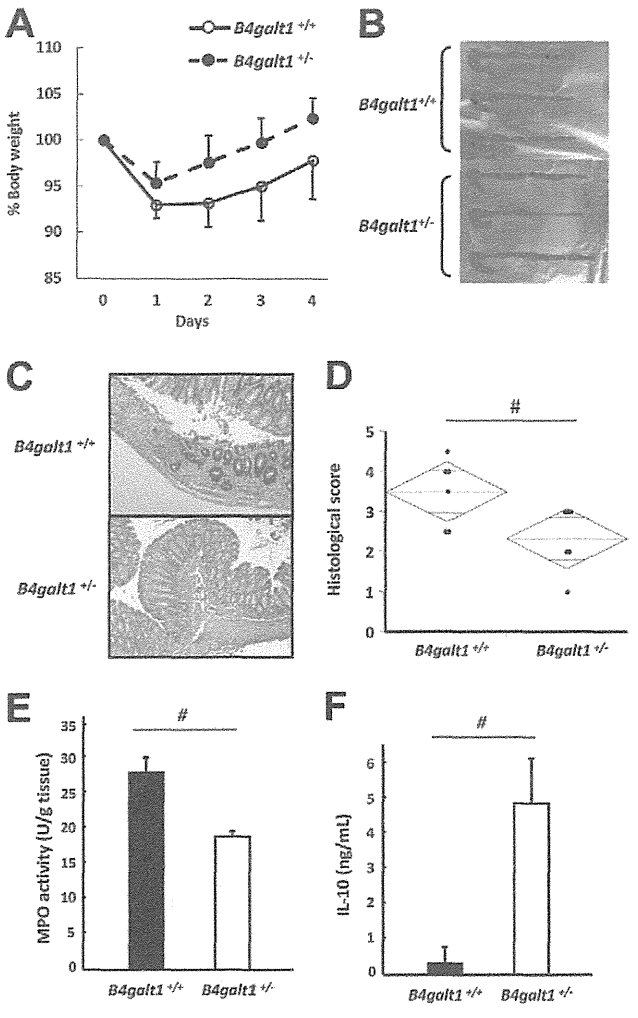

Figure 4. Amelioration of TNBS-induced colitis in *B4galt1*$^{+/-}$ mice. (*A*) Body weight of *B4galt1*$^{+/+}$ and *B4galt1*$^{+/-}$ mice subjected to TNBS-induced colitis. (*B*) Macroscopic pictures of the colons from *B4galt1*$^{+/+}$ and *B4galt1*$^{+/-}$ mice. (*C*) Representative micrographs of H&E-stained colon. (*D*) Histological scores of TNBS colitis in *B4galt1*$^{+/+}$ and *B4galt1*$^{+/-}$ mice. (*E*) Myeloperoxidase activity of the colons from *B4galt1*$^{+/+}$ and *B4galt1*$^{+/-}$ mice. (*F*) IL-10 production of colonic LP mononuclear cells in *B4galt1*$^{+/+}$ and *B4galt1*$^{+/-}$ mice. Data are shown as mean ± standard error of mean of 6 mice per group. $^{\#}P < .05$.

results indicate that IL-10 is indispensable for the protection of colitis in *B4galt1*$^{+/-}$ mice.

B4galt1$^{+/-}$ B Cells Have a Protective Role in the CD4^{+}CD62L^{+} T-Cell Transfer Colitis Model

To explore the function of agalactosyl IgG in murine colitis, IgG purified from the sera (40 μg) of *B4galt1*$^{+/-}$ and *B4galt1*$^{+/+}$ mice were injected intraperitoneally into C57BL/6 mice at day 0 of DSS administration. Consistent with previous reports,[7,20] injection of IgG improved DSS-induced colitis compared to mice injected with phosphate-buffered saline. The severity of colitis, however, did not differ significantly between mice injected with IgG purified from *B4galt1*$^{+/-}$ and *B4galt1*$^{+/+}$ mice (Supplementary Figure 2*A, B,* and *C*). IL-10 production in the SP was also unchanged between mice injected with *B4galt1*$^{+/-}$ and *B4galt1*$^{+/+}$ IgG (Supplementary Figure 2*D*). The severity of colitis was unchanged even when we increased the dose of IgG to 1 mg/mouse (data not shown). These findings indicate that agalactosylation of IgG itself does not have a protective role against colitis.

We next examined whether oligosaccharide alterations of glycoproteins on B cells affect B cell function in *B4galt1*$^{+/-}$ mice. Colitis was generated in *Rag2*$^{-/-}$ mice, which do not develop B and T cells, by the adoptive transfer of CD4^{+}CD62L^{+} cells isolated from C57BL/6 mice. MLN B cells isolated from *B4galt1*$^{+/-}$ or *B4galt1*$^{+/+}$ mice were also cotransferred to the mice. We confirmed the transfer of B cells into *Rag2*$^{-/-}$ mice using immunohistochemical analysis of B220-positive cells and analysis of serum IgG oligosaccharides after adoptive transfer (Supplementary Figure 4*A, B*). Mice that received CD4^{+}CD62L^{+} T cells and B cells from *B4galt1*$^{+/-}$ mice had significantly decreased body-weight loss compared to mice transferred with CD4^{+}CD62L^{+} T cells with/without B cells from *B4galt1*$^{+/+}$ mice (Figure 6*A*). The histologic score was similar between mice transferred with CD4^{+}CD62L^{+} T cells together with B cells from *B4galt1*$^{+/-}$ mice and mice transferred with CD4^{+}CD62L^{+} T cells alone. In contrast, mice transferred with B cells from *B4galt1*$^{+/-}$ mice and CD4^{+}CD62L^{+} T cells exhibited significantly less severe colitis than mice transferred with CD4^{+}CD62L^{+} T cells alone (Figure 6*B, C*). In addition, IL-10 production from the SP of mice transferred with *B4galt1*$^{+/-}$ B cells was significantly higher than that of mice transferred with *B4galt1*$^{+/+}$ B cells (Figure 6*D*). IL-10 production from the LP of mice transferred with *B4galt1*$^{+/-}$ B cells tended to be higher than that transferred with *B4galt1*$^{+/+}$ B cells (Figure 6*E*). These findings show that MLN B cells from *B4galt1*$^{+/-}$ mice protect against colitis more effectively than B cells from *B4galt1*$^{+/+}$ mice.

Cell-to-Cell Communication Between B4galt1$^{+/-}$ B Cells and Macrophages via Galectin Is Required for Production of IL-10

Although B cells from *B4galt1*$^{+/-}$ mice protect against colitis (Figure 6), a difference of IL-10 production between *B4galt1*$^{+/-}$ mice and *B4galt1*$^{+/+}$ mice was observed in CD11b^{+} macrophages, but not in B cells (Figure 3*D*). We then tested the possibility that IL-10 is produced from macrophages by interactions with B cells of *B4galt1*$^{+/-}$ mice. MLN B cells from *B4galt1*$^{+/-}$ and *B4galt1*$^{+/+}$ mice were cocultured with MLN macrophages from *B4galt1*$^{+/+}$ mice in the presence of LPS. IL-10 production was significantly increased when macrophages were cocultured with B cells from *B4galt1*$^{+/-}$ mice compared with B cells from *B4galt1*$^{+/+}$ mice (Figure 7*A*). To explore whether direct cell-to-cell interactions of the 2 cell types is necessary for the production of IL-10, B cells and macrophages were cultured in a Transwell system. IL-10 production was severely impaired by blocking the cell–cell contact of B cells and macrophages (Figure 7*A*). Monoculture of B cells

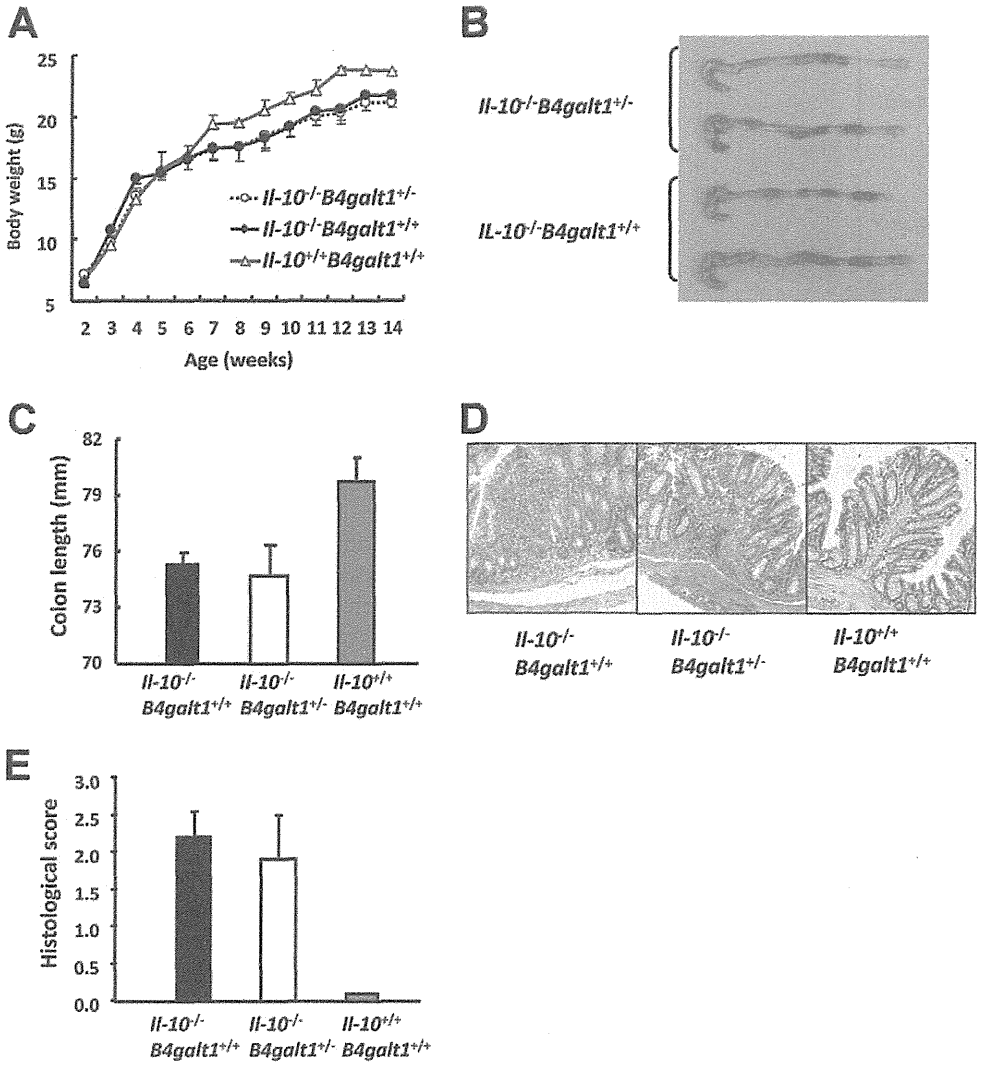

Figure 5. Amelioration of colitis in *B4galt1*$^{+/-}$ mice was blocked by IL-10 deficiency. (*A*) Mean (±standard error of mean) body weight of *Il-10*$^{-/-}$*B4galt1*$^{+/+}$, *Il-10*$^{-/-}$*B4galt1*$^{+/-}$, and *Il-10*$^{+/+}$*B4galt1*$^{+/+}$ mice. (*B*) Macroscopic pictures of colons from *IL-10*$^{-/-}$*B4galt1*$^{+/+}$ and *Il-10*$^{-/-}$*B4galt1*$^{+/-}$ mice at 14 weeks of age. Colon length (*C*), representative micrographs of the colon (*D*), and histologic scores of the colon (*E*) of mice in *Il-10*$^{-/-}$*B4galt1*$^{+/+}$, *IL-10*$^{-/-}$*B4galt1*$^{+/-}$, and *Il-10*$^{+/+}$*B4galt1*$^{+/+}$ mice at 14 weeks of age (n = 8/group). Data are shown as mean ± standard error of mean.

or macrophages did not induce IL-10 production (Figure 7*A*). These results indicate that cell-to-cell communication between B cells and macrophages with decreased B4GalTI activity contributes to IL-10 production.

We next tested the possibility that oligosaccharides other than galactose are altered, thereby altering the immune response in *B4galt1*$^{+/-}$ MLN B cells. Lectin microarray was performed to compare the oligosaccharide profiles of *B4galt1*$^{+/-}$ and *B4galt1*$^{+/+}$ MLN B cells and macrophages. Consistent with the expected pharmacokinetics of B4GalTI deficiency, both *B4galt1*$^{+/-}$ B cells and macrophages had significantly lower affinity to *Erythrina cristagalli* agglutinin and *Ricinus communis* agglutinin 120, which bind to galactose rather than *B4galt1*$^{+/+}$ B cells. In addition, *B4galt1*$^{+/-}$ B cells had significantly higher affinity to DSA and *Lycopersicon esculentum* lectin, which recognize polylactosamine[21] compared with *B4galt1*$^{+/+}$ B cells (Figure 7*B*, Supplementary Figure 5). These findings were confirmed by flow cytometric analysis of *B4galt1*$^{+/-}$ B cells, which exhibit higher affinity to DSA than *B4galt1*$^{+/+}$ B cells. In contrast, affinity to *Ricinus communis* agglutinin 120 was lower in *B4galt1*$^{+/-}$ B cells than in *B4galt1*$^{+/+}$ B cells (Figure 7*C*). These results showed that polylactosamine structures are increased on *B4galt1*$^{+/-}$ B cells. In addition to the changes in B cells, *B4galt1*$^{+/-}$ macrophages had significantly higher affinity to DSA and *Lycopersicon esculentum* lectin than *B4galt1*$^{+/+}$ macrophages (Figure 7*B*). Because polylactosamine tightly binds to galectins,[22] we next investigated the possibility that galectin is involved in cell-to-cell communication. When macrophages and B cells were preincubated with lactose, which inhibits interaction via galectins, IL-10 production in the coculture of macrophages and *B4galt1*$^{+/-}$ B cells was significantly decreased in the presence of lactose compared with the control (Figure 7*D*). When macrophages from *B4galt1*$^{+/-}$ mice were stimulated with galectins, galectin-1, but not galectin-3 or 4, induced significantly higher amount of IL-10 production from *B4galt1*$^{+/-}$ macrophages than *B4galt1*$^{+/+}$ macrophages (Figure 7*E*).

Discussion

The findings of the present study indicate *B4galt1*-deficient mice are protected from colitis. In addition,

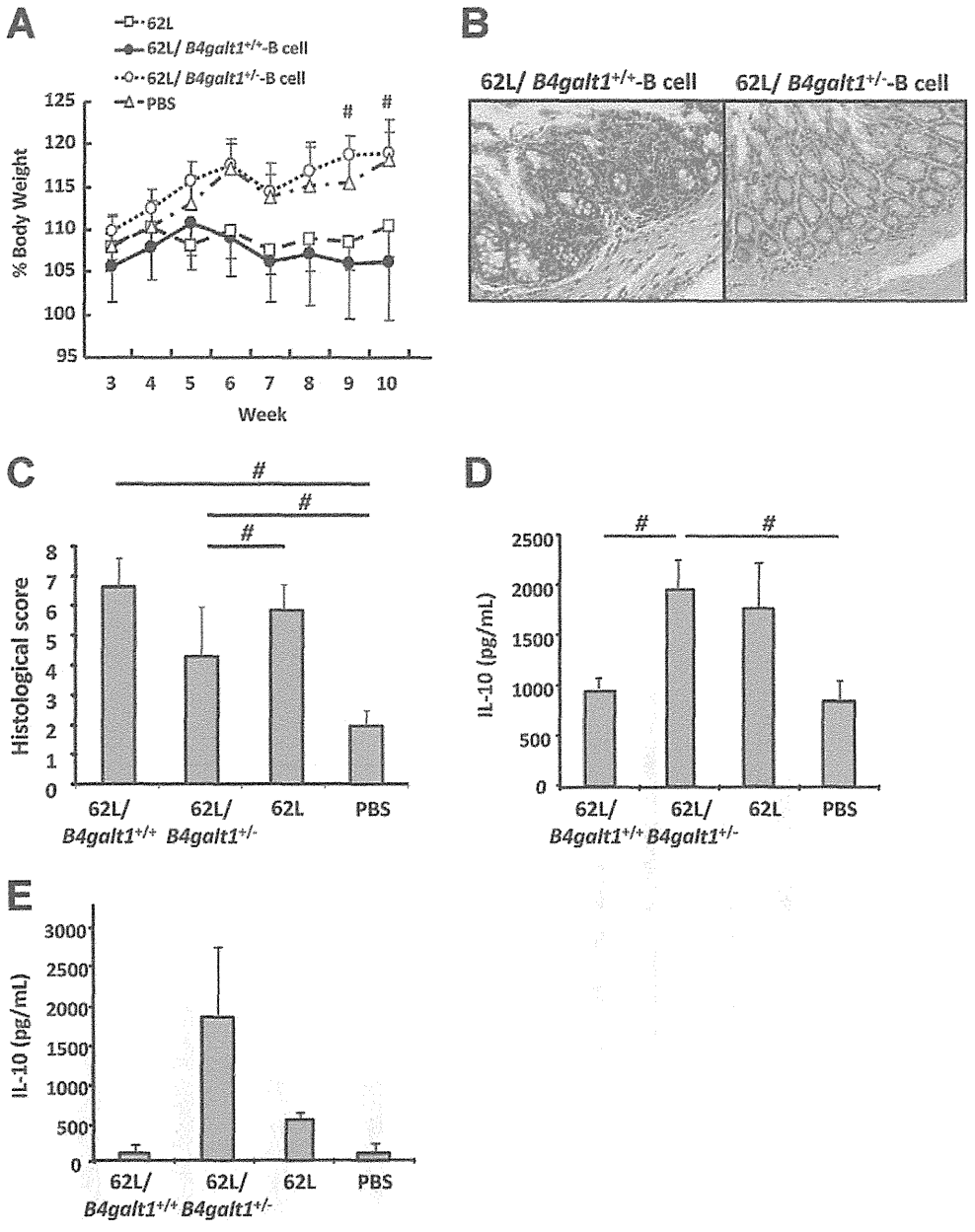

Figure 6. Adoptive transfer of B cells isolated from *B4galt1*$^{+/-}$ mice ameliorated colitis in *Rag2*$^{-/-}$ mice transferred with CD4^{+}CD62L^{+} T cells. (*A*) Mean (±standard error of mean) body weight loss in mice transferred with B cells from *B4galt1*$^{+/+}$ mice together with CD4^{+}CD62L^{+} T cells (62L/*B4galt1*$^{+/+}$) was not significantly different from that in mice transferred with CD4^{+} CD62L^{+} T cells alone (62L). Mice transferred with B cells from *B4galt1*$^{+/-}$ mice and CD4^{+} CD62L^{+} T cells (62L/*B4galt1*$^{+/-}$) had significantly less body-weight loss than mice transferred with CD4^{+}CD62L^{+} T cells alone ($^{\#}P <$ .05). (*B*) Representative micrographs of colons of 62L/ *B4galt1*$^{+/+}$ and 62L/*B4galt1*$^{+/-}$ mice. (*C*) Histologic colitis scores of 62L/*B4galt1*$^{+/-}$ mice were significantly lower than those of 62L/ *B4galt1*$^{+/+}$ mice. (*D*) IL-10 production in the spleen isolated from 62L/*B4galt1*$^{+/-}$ mice was significantly higher (P = .010) than that isolated from 62L/*B4galt1*$^{+/+}$ mice. (*E*) IL-10 production in the cells of colonic LP with or without adoptive transfer. Data are shown as mean ± standard error of mean of 10 mice per group. $^{\#}P <$ .05.

B4galt1-deficient B cells have important roles in the amelioration of colitis by inducing IL-10 production from macrophages.

Several reports suggest that IgG oligosaccharide alterations modulate immune functions, such as augmentation of antibody-dependent cellular cytotoxicity by the absence of fucose[23] or anti-inflammatory effects by the terminal sialic acid.[24] In addition to the IgG oligosaccharide changes in fucose and sialic acid, agalactosyl IgG can also modulate the immune response to cause pathogenicity in murine arthritis models.[25] In the present study, however, the severity of colitis was unchanged by the passive transfer of agalactosyl IgG compared with the transfer of fully galactosyl IgG (Supplementary Figure 2). The effect of agalactosyl IgG can differ between colitis and arthritis models due to the lack of a specific autoantibody, or due to the difference in the contribution of antibodies between colitis and arthritis disease models.

We initially expected that *B4galt1*$^{+/-}$ mice would develop more severe DSS- and TNBS-induced colitis because *B4galt1*$^{+/-}$ mice have a deficiency of galactose in IgG oligosaccharides similar to that of patients with CD. *B4galt1*$^{+/-}$ mice, however, were protected from colitis. IL-10 production from CD11b^{+} cells was significantly increased in *B4galt1*$^{+/-}$ mice compared with *B4galt1*$^{+/+}$ mice. The importance of IL-10 for the prevention of colitis in *B4galt1*$^{+/-}$ mice was further confirmed by the finding that colitis was not ameliorated in *Il-10*$^{-/-}$*B4galt1*$^{+/-}$ mice. The protective role of IL-10 is well established in colitis models.[26] IL-10 is induced by T cells, B cells, and by macrophages via several cascades, such as Fcγ receptor ligation, CD40 ligation, and stimulation via Toll-like re-

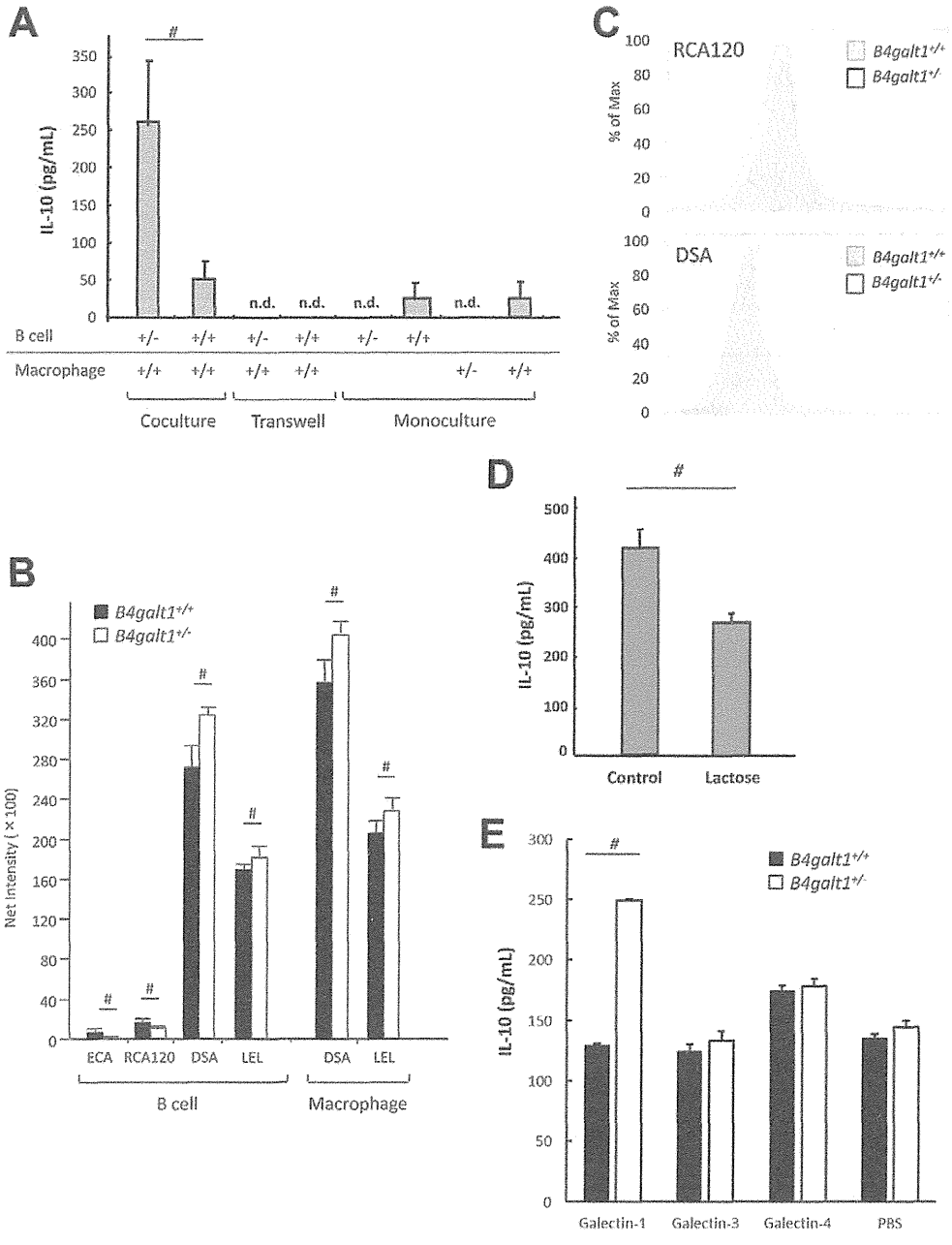

Figure 7. IL-10 production from macrophages of *B4galt1*$^{+/+}$ mice was stimulated in the presence of B cells from *B4galt1*$^{+/-}$ mice. (*A*) IL-10 production in coculture of MLN B cells and macrophages. CD11b^{+} macrophages from MLN of *B4galt1*$^{+/+}$ mice and CD19^{+} B cells from MLN of *B4galt1*$^{+/+}$ mice or *B4galt1*$^{+/-}$ mice (2×10^5 cells each) were cultured as coculture, Transwell culture, or monoculture with LPS for 48 hours. Culture supernatants were collected and cytokine production was calculated by enzyme-linked immunosorbent assay. (*B*) Lectin microarray analysis. Cellular proteins derived from CD19^{+} B cells or CD11b^{+} macrophages from *B4galt1*$^{+/+}$ mice or *B4galt1*$^{+/-}$ mice were applied where lectins were immobilized in triplicate. $^{\#}P < .05$. (*C*) Lectin flow cytometry analysis for DSA and *Ricinus communis* agglutinin 120 (RCA120). Representative histograms for RCA120 or DSA expression gated in CD19-positive cells in 3 separate experiments are shown. (*D*) IL-10 production in coculture of *B4galt1*$^{+/+}$ macrophages and *B4galt1*$^{+/-}$ B cells with lactose. Both cells were preincubated with 20 mM lactose or control sugar (sucrose) for 1 hour and cocultured in the presence of LPS for 48 hours. (*E*) IL-10 production in *B4galt1*$^{+/+}$ and *B4galt1*$^{+/-}$ macrophages stimulated with 5 μg/mL recombinant galectin-1, 3, or 4 or phosphate-buffered saline for 48 hours. Data are shown as mean ± standard error of mean of 4 independent experiments. $^{\#}P < .05$.

ceptors.[27-29] IL-10 released from CD11b^{+} myeloid cells, perhaps mostly macrophages, acts on regulatory T cells to maintain Foxp3 expression and suppress murine colitis.[30] Thus, IL-10 produced from CD11b^{+} macrophages can have multiple functions to suppress inflammation in *B4galt1*$^{+/-}$ mice. Agalactosylation of immune cells in IBD might serve to maintain homeostasis in the gut to inhibit excessive inflammation.

Lectin microarray and flow cytometry showed that *B4galt1*$^{+/-}$ B cells and macrophages exhibit high affinities to lectins that recognize polylactosamine chains. The reason for the increased surface expression of polylactosamine in *B4galt1*$^{+/-}$ cells is unknown, but our results are consistent with that of a previous report showing that polylactosamine is overexpressed on erythrocytes isolated from *B4galt1*$^{-/-}$ mice.[31] We also demonstrated that lactose, a galectin inhibitor, blocks IL-10 production induced by cell-to-cell communication between B cells and macrophages.[16] The galectins are a family of soluble animal lectins that carry a carbohydrate-recognition domain. Different galectins have distinct specificities for oligosaccharides. Galectin-1 is constitutively expressed in lymphoid organs[32] and has anti-inflammatory properties for the protection of murine colitis.[33] Galectin-1 binds tightly to the polylactosamine chains that are commonly found on the cell surface proteins via 2 identical carbohydrate-recognition domains, thereby building a lattice formation by cross linking 2 polylactosamines and modulating cellular function.[22] Remarkably, galectin-1 enhances IL-10 production.[34] In

the present study, IL-10 production by coculture of B cells and macrophages was inhibited by lactose, and stimulation of galectin-1 on macrophages up-regulated IL-10 production, suggesting that galectin-1 cross links polylactosamines on B cells and macrophages and mediates IL-10 production from macrophages. The expression of galectin-1, however, did not differ between *B4galt1*$^{+/-}$ and *B4galt1*$^{+/+}$ B cells (data not shown). The expression of galectin-9, which also induces IL-10 production,[35] was unchanged between *B4galt1*$^{+/-}$ and *B4galt1*$^{+/+}$ B cells (data not shown). In addition, IL-10 production was not completely inhibited by lactose (Figure 7*D*). These findings suggest that molecules other than galectin-1 might be involved in the IL-10 production. Additional studies are necessary to clarify the polylactosamine carrier molecules that contribute to alter cytokine responses after contact between these 2 cell types.

We also tested other molecules to explain the enhanced production of IL-10 by the interaction of B cells and macrophages in *B4galt1*$^{-/-}$ mice. *B4galt1*$^{-/-}$ mice have impaired inflammatory responses and are defective in selectin-ligand biosynthesis.[18] Although the levels of selectin-ligand were impaired in *B4galt1*$^{-/-}$ mice, the levels of selectin-ligand in B cells or macrophages determined using a chimeric P-selectin IgM molecule were not different between *B4galt1*$^{+/-}$ and *B4galt1*$^{+/+}$ mice (data not shown). Therefore, the interaction between selectin and selectin ligand on B cells and macrophages was not considered to be altered in *B4galt1*$^{+/-}$ mice. We also tested the expression of other negative costimulatory molecules, such as inducible costimulatory molecule and T-cell inhibitory receptor programmed death-1;[36] no differences in their expression were observed between *B4galt1*$^{+/-}$ and *B4galt1*$^{+/+}$ mice (data not shown).

In summary, *B4galt1*-deficient B cells and macrophages act to protect against murine experimental colitis by producing anti-inflammatory cytokines such as IL-10. Colitis was ameliorated by the modulation of oligosaccharides in the murine models of colitis and the induction of alterations in oligosaccharides has potential therapeutic efficacy in IBD.

Supplementary Material

Note: To access the supplementary material accompanying this article, visit the online version of *Gastroenterology* at www.gastrojournal.org, and at doi: 10.1053/j.gastro.2012.02.008.

References

1. Shanahan F. Crohn's disease. Lancet 2002;359:62–69.
2. Shinzaki S, Iijima H, Nakagawa T, et al. IgG oligosaccharide alterations are a novel diagnostic marker for disease activity and the clinical course of inflammatory bowel disease. Am J Gastroenterol 2008;103:1173–1181.
3. Sox HC Jr, Hood L. Attachment of carbohydrate to the variable region of myeloma immunoglobulin light chains. Proc Natl Acad Sci U S A 1970;66:975–982.
4. Mizuochi T, Taniguchi T, Shimizu A, et al. Structural and numerical variations of the carbohydrate moiety of immunoglobulin G. J Immunol 1982;129:2016–2020.
5. Keusch J, Lydyard PM, Delves PJ. The effect on IgG glycosylation of altering beta1, 4-galactosyltransferase-1 activity in B cells. Glycobiology 1998;8:1215–1220.
6. Mizoguchi A, Mizoguchi E, Smith RN, et al. Suppressive role of B cells in chronic colitis of T cell receptor alpha mutant mice. J Exp Med 1997;186:1749–1756.
7. Levine DS, Fischer SH, Christie DL, et al. Intravenous immunoglobulin therapy for active, extensive, and medically refractory idiopathic ulcerative or Crohn's colitis. Am J Gastroenterol 1992; 87:91–100.
8. Asano M, Furukawa K, Kido M, et al. Growth retardation and early death of beta-1,4-galactosyltransferase knockout mice with augmented proliferation and abnormal differentiation of epithelial cells. EMBO J 1997;16:1850–1857.
9. Iijima H, Neurath MF, Nagaishi T, et al. Specific regulation of T helper cell 1-mediated murine colitis by CEACAM1. J Exp Med 2004;199:471–482.
10. Mudter J, Wirtz S, Galle PR, et al. A new model of chronic colitis in SCID mice induced by adoptive transfer of CD62L+ CD4+ T cells: insights into the regulatory role of interleukin-6 on apoptosis. Pathobiology 2002;70:170–176.
11. Dohi T, Ejima C, Kato R, et al. Therapeutic potential of follistatin for colonic inflammation in mice. Gastroenterology 2005;128: 411–423.
12. Berg DJ, Davidson N, Kuhn R, et al. Enterocolitis and colon cancer in interleukin-10-deficient mice are associated with aberrant cytokine production and CD4(+) TH1-like responses. J Clin Invest 1996;98:1010–1020.
13. Liu Z, Geboes K, Colpaert S, et al. Prevention of experimental colitis in SCID mice reconstituted with CD45RBhigh CD4+ T cells by blocking the CD40-CD154 interactions. J Immunol 2000;164: 6005–6014.
14. Nakajima S, Iijima H, Shinzaki S, et al. Functional analysis of agalactosyl IgG in inflammatory bowel disease patients. Inflamm Bowel Dis 2011;17:927–936.
15. Aicher WK, Fujihashi K, Yamamoto M, et al. Effects of the lpr/lpr mutation on T and B cell populations in the lamina propria of the small intestine, a mucosal effector site. Int Immunol 1992;4: 959–968.
16. Stowell S, Arthur C, Dias-Baruffi M, et al. Innate immune lectins kill bacteria expressing blood group antigen. Nat Med 2010;16: 295–301.
17. Kuno A, Uchiyama N, Koseki-Kuno S, et al. Evanescent-field fluorescence-assisted lectin microarray: a new strategy for glycan profiling. Nat Methods 2005;2:851–856.
18. Asano M, Nakae S, Kotani N, et al. Impaired selectin-ligand biosynthesis and reduced inflammatory responses in beta-1,4-galactosyltransferase-I-deficient mice. Blood 2003;102:1678–1685.
19. Kuhn R, Lohler J, Rennick D, et al. Interleukin-10-deficient mice develop chronic enterocolitis. Cell 1993;75:263–274.
20. Shintani N, Nakajima T, Nakakubo H, et al. Intravenous immunoglobulin (IVIG) treatment of experimental colitis induced by dextran sulfate sodium in rats. Clin Exp Immunol 1997;108:340–345.
21. Carlsson S, Fukuda M. The polylactosaminoglycans of human lysosomal membrane glycoproteins lamp-1 and lamp-2. Localization on the peptide backbones. J Biol Chem 1990;265:20488–20495.
22. Camby I, Le Mercier M, Lefranc F, et al. Galectin-1: a small protein with major functions. Glycobiology 2006;16:137R–157R.
23. Shinkawa T, Nakamura K, Yamane N, et al. The absence of fucose but not the presence of galactose or bisecting N-acetylglucosamine of human IgG1 complex-type oligosaccharides shows the critical role of enhancing antibody-dependent cellular cytotoxicity. J Biol Chem 2003;278:3466–3473.

24. Kaneko Y, Nimmerjahn F, Ravetch JV. Anti-inflammatory activity of immunoglobulin G resulting from Fc sialylation. Science 2006; 313:670–673.
25. Rademacher TW, Williams P, Dwek RA. Agalactosyl glycoforms of IgG autoantibodies are pathogenic. Proc Natl Acad Sci U S A 1994;91:6123–6127.
26. Kühn R, Löhler J, Rennick D, et al. Interleukin-10-deficient mice develop chronic enterocolitis. Cell 1993;75:263–274.
27. Gordon S. Alternative activation of macrophages. Nat Rev Immunol 2003;3:23–35.
28. Edwards JP, Zhang X, Frauwirth KA, et al. Biochemical and functional characterization of three activated macrophage populations. J Leukoc Biol 2006;80:1298–1307.
29. Boonstra A, Rajsbaum R, Holman M, et al. Macrophages and myeloid dendritic cells, but not plasmacytoid dendritic cells, produce IL-10 in response to MyD88- and TRIF-dependent TLR signals, and TLR-independent signals. J Immunol 2006;177:7551–7558.
30. Murai M, Turovskaya O, Kim G, et al. Interleukin 10 acts on regulatory T cells to maintain expression of the transcription factor Foxp3 and suppressive function in mice with colitis. Nat Immunol 2009;10:1178–1184.
31. Kotani N, Asano M, Inoue N, et al. Polylactosamine synthesis and branch formation of N-glycans in beta1,4-galactosyltransferase-1-deficient mice. Arch Biochem Biophys 2004;426: 258–265.
32. Barondes S, Castronovo V, Cooper D, et al. Galectins: a family of animal beta-galactoside-binding lectins. Cell 1994;76:597–598.
33. Santucci L, Fiorucci S, Rubinstein N, et al. Galectin-1 suppresses experimental colitis in mice. Gastroenterology 2003;124:1381–1394.
34. van der Leij J, van den Berg A, Harms G, et al. Strongly enhanced IL-10 production using stable galectin-1 homodimers. Mol Immunol 2007;44:506–513.
35. Kim J, Cho M, Choi S, et al. Inhibition of dextran sulfate sodium (DSS)-induced intestinal inflammation via enhanced IL-10 and TGF-beta production by galectin-9 homologues isolated from intestinal parasites. Mol Biochem Parasitol 2010;174:53–61.
36. Greenwald RJ, Latchman YE, Sharpe AH. Negative co-receptors on lymphocytes. Curr Opin Immunol 2002;14:391–396.

Received January 15, 2011. Accepted February 8, 2012.

Reprint requests

Address requests for reprints to: Hideki Iijima, MD, PhD, Department of Gastroenterology and Hepatology, Osaka University Graduate School of Medicine, 2-2 K1 Yamadaoka, Suita, Osaka 565-0871, Japan. e-mail: hiijima@gh.med.osaka-u.ac.jp; fax: (+81) 6-6879-3629.

Acknowledgments

The authors thank Drs Masayuki Miyasaka and Takako Hirata (Osaka University) for providing the chimeric P-selectin IgM molecule. The authors also thank Dr Richard S. Blumberg (Harvard Medical School) for helpful comments.

The manuscript was edited by SciTechEdit International, LLC (Highlands Ranch, CO) with the funding of Grant-in-Aid from the Japan Society for the Promotion of Science.

Shinichiro Shinzaki, Hideki Iijima, and Hironobu Fujii contributed equally.

Conflicts of interest

This author discloses the following: Shunsaku Takeishi is an employee of GP BioScience Ltd. The remaining authors disclose no conflicts.

Funding

This work was supported by a Grant-in-Aid for Scientific Research no. 21249038, a Grant-in-Aid for Scientific Research no. 19590721, and a Grant-in-Aid for Young Scientists no. 22790643, from the Japan Society for the Promotion of Science; a grant from the Global COE program of Osaka University funded by the Ministry of Education, Culure, Sports, Science, and Technology of Japan; and a Grant-in-Aid from the Smoking Research Foundation.

Journal of proteome research

Article

pubs.acs.org/jpr

Analysis of Polarized Secretion of Fucosylated Alpha-Fetoprotein in HepG2 Cells

Tsutomu Nakagawa,[†] Kenta Moriwaki,[†] Naoko Terao,[†] Takatoshi Nakagawa,[‡] Yasuhide Miyamoto,[§] Yoshihiro Kamada,[†] and Eiji Miyoshi*[,†]

[†]Department of Molecular Biochemistry and Clinical Investigation, Osaka University Graduate School of Medicine, Osaka, Japan

[‡]Department of Pharmacology, Osaka Medical College, Osaka, Japan

[§]Department of Immunology, Osaka Medical Center for Cancer and Cardiovascular Diseases, Osaka, Japan

ABSTRACT: Fucosylated alpha-fetoprotein (AFP) is a more specific biomarker for hepatocellular carcinoma (HCC) than AFP. However, the mechanisms underlying the increase in fucosylated AFP in sera of HCC patients remain largely unknown. Recently, we reported that fucosylation is a possible signal for the secretion of hepatic glycoproteins into bile and that the fucosylation-based sorting machinery might be disrupted in the liver bearing HCC. In this study, we investigated the selective secretion of fucosylated AFP into bile canaliculus (BC) structures of the human hepatoma cell line HepG2. The proportion of fucosylated AFP in BC structures was higher than that in the medium, as judged by lectin affinity electrophoresis. Suppression of fucosylation by the double knock-down of GDP-mannose-4,6-dehydratase and the human homologue of GDP-4-keto-6-deoxymannose-3,5-epimerase-4-reductase, which contribute to the synthesis of GDP-fucose, a donor substrate for fucosyltransferases, did not decrease the proportion of fucosylated AFP in BC structures but decreased this proportion in conditioned medium. Furthermore, increased AFP fucosylation was observed in medium, but not in BC structures, upon adding free fucose. These results suggest that saturation of fucosylated AFP in BC structures is accompanied by its increase in conditioned medium, probably leading to increased fucosylated AFP in sera of HCC patients.

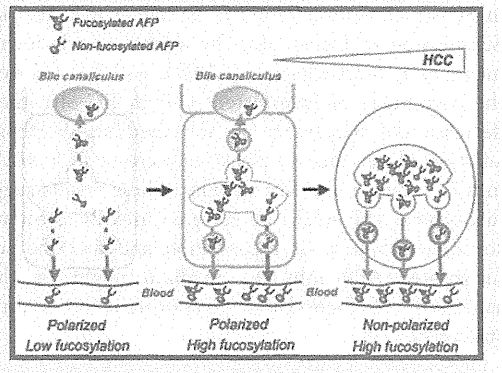

KEYWORDS: *AFP-L3, fucose, bile canaliculus, HepG2 cells*

INTRODUCTION

Alpha-fetoprotein (AFP) is an oncofetal glycoprotein that contains a single *N*-glycosylation site,[1] and its oligosaccharide structure varies with developmental stage and disease state.[2−4] Fucosylated AFP, referred to as the L3 fraction of AFP (AFP-L3), is a highly specific tumor marker for hepatocellular carcinomas (HCC). Increases in serum AFP levels are observed in patients with chronic liver diseases such as liver cirrhosis, but fucosylated AFP is scarcely detected in benign liver disease.[5] The majority of the oligosaccharide structures of AFP-L3 are alpha1−6 fucosylated biantennary structures.[4] Alpha1−6 fucosyltransferase (Fut8) is involved in the fucosylation of AFP, and we previously succeeded in the purification and cDNA cloning of Fut8 from porcine brain[6] and a human gastric cancer cell line.[7] Whereas overexpression of Fut8 in Hep3B cells increased the rate of fucosylation of AFP, high expression of Fut8 was observed in noncancerous liver cirrhotic tissues as well as in HCC tissues.[8] Therefore, other factors must be linked to the specific incidence of fucosylated AFP in HCC. GDP-fucose is a donor substrate for Fut8. When we determined the GDP-fucose levels in liver tissues, using an assay for GDP-fucose levels in cells/tissues, the levels in HCC tissues were found to be significantly higher than those in cirrhotic and normal liver tissues.[9,10] The increase in GDP-fucose in HCC is due to the enhanced expression of the human homologue of GDP-4-keto-6-deoxymannose-3,5-epimerase-4-reductase (FX), which contributes to the synthesis of GDP-fucose.[11] Therefore, both Fut8 and FX would regulate the production of fucosylated AFP in HCC. However, Fut8 and FX were increased 2- to 3-fold in HCC tissues compared to the surrounding tissues, and thus another factor must be involved in terms of an increase in fucosylated AFP in the sera of HCC patients.

Hepatocytes, the major epithelial cells in the liver, produce a variety of serum glycoproteins and nonglycosylated proteins including albumin. There are two secretion pathways in hepatocytes. One pathway involves secretion to the apical surface of hepatocytes, which is followed by secretion into bile ducts. The other involves secretion to the basolateral surface, which is followed by secretion into blood vessels. Interestingly, it is reported that common serum proteins including albumin are detected in bile.[12] The molecular and cellular mechanisms for the secretion pathway are intensively investigated topics, but remain largely unknown.

Recently, we reported that many glycoproteins in bile were strongly fucosylated, compared to those in serum, and

Received: November 22, 2011
Published: April 9, 2012

suggested that fucosylation might be a possible signal for the secretion of glycoproteins into bile.[13] Further, we found that the sorting machinery via fucosylation might be disrupted in a rodent HCC model.[14] The question therefore arises whether fucosylated AFP is also regulated by this common fucosylation sorting system.

In this study, to investigate the polarized secretion of fucosylated AFP in the HCC liver, we used human hepatocarcinoma (HepG2) cells, which form bile canaliculus (BC) structures[15,16] and produce fucosylated AFP. Polarized HepG2 cells have been proven to be a suitable model for the study of several functional properties of normal hepatocytes, including metabolism, sorting, polarized transport, and secretion.[17] Glycoproteins secreted into BC structures and the culture medium are equivalent to biliary and serum glycoproteins, respectively. The percentage of fucosylated AFP in BC structures was found to be higher than that in medium. Suppression of fucosylation by double knock-down of GDP-mannose-4, 6-dehydratase (GMD), and FX did not decrease the percentage of fucosylated AFP in BC structures but did decrease the percentage in the medium. Furthermore, the addition of free fucose caused an increase in fucosylation only in AFP secreted into the medium. These results suggested that fucosylated AFP might be secreted into BC structures by the sorting machinery via fucosylation and that the secretion of fucosylated AFP into the medium might be due to the saturation of fucosylated glycoprotein secretion into BC structures.

EXPERIMENTAL SECTION

Reagents

Biotinated AOL (*Aspergillus oryzae*) was purchased from Tokyo Kasei Kogyo Co., Ltd. (Tokyo, Japan). Fucose was from Sigma (St Louis, MO).

Cell Cultures

Cells of the human HCC cell line HepG2 (American Type Culture Collection, Rockville, MD) were cultured in Dulbecco's modified Eagle's medium containing 4.5 g/L of glucose supplemented with 10% fetal bovine serum (FBS), 100 U/mL of penicillin G, and 100 μg/mL of streptomycin in a humidified atmosphere of 5% CO_2 at 37 °C. The formation of BC structures was confirmed by immunostaining for canalicular membrane proteins such as multidrug resistance protein 1, tight junction associated protein, Zonula occludens 1, and actin filaments, with confocal microscopy (data not shown).

The collection of proteins secreted into BC structures was performed by means of the modified method described by Bastaki et al.[18] Briefly, HepG2 cells were seeded at 2.5×10^3 cells/cm^2 on collagen type I-coated dishes (Iwaki, Chiba, Japan) and cultured for 4 days. After the cells were rinsed twice with medium without FBS, the cells were cultured in medium without FBS for 1 day. The medium was collected, and then the cells were incubated twice with 2.5 mM EGTA, 50 mM 2-deoxyglucose, and 5 mM NaN_3 for 15 min at 37 °C to disrupt the tight junctions, thereby releasing the proteins secreted into BC structures. We confirmed that actin, a major cytosolic protein, was not contained in the material from BC structures to deny a possibility of cell damages followed by a release of cellular proteins (data not shown).

Establishment of GMD and FX Double Knock-Down Cell Lines

GMD and FX double knock-down (DKD) cell lines were established by retroviral introduction of small hairpin RNA (shRNA) against the *GMDS* and *FX* genes. Briefly, retroviral expression vectors designed to express shRNA targeted to the *GMDS* and *FX* genes were constructed as follows. A 19-nucleotide sequence of the *GMDS* and *FX* genes was inserted in the sense and antisense directions into the pSINsi-hU6 DNA vector (Takara Bio Inc., Shiga, Japan) and RNAi-Ready pSIREN-RetroQ vector (Promega, Madison, WI) containing the human U6 promoter, respectively. The shRNA for *GMDS* was designed to form 19-bp dsRNA with 2 thymine overhangs at both 3′ ends. The targeting sequences of the *GMDS* and *FX* siRNAs used are as follows. *GMDS*, sense: 5′-CGACUUCUA-GAUGCAGUUATT-3′, antisense: 3′-TTGCUGAAGAU-CUACGUCAAU; *FX*, sense: 5′-GAAGUCACCUUUGAUA-CAA-3′, antisense: 5′-CUUCAGUGGAAACUAUGUU-3′. Recombinant retroviruses were generated by cotransfection of a vector mixture, such as the recombinant retrovirus vector, pE-ampho vector (Amphotropic *env*), and the pGP vector (*gag-pol*) into human embryonic kidney 293 cells. Recombinant retrovirus particles containing the target sequences of *GMDS* and *FX* genes were infected into HepG2 cells, and the Geneticin (G418)-resistant clones for GMD and puromycin-resistant clones for FX were selected as stable transfectants.

Lectin Blot Analysis

Lectin blot analysis was performed as described previously.[19] Briefly, 5 μg of proteins were subjected to 12% sodium dodecylsulfate-polyacrylamide gel electrophoresis (SDS-PAGE). After the electrophoresis, the gel was blotted onto a nitrocellulose membrane. The membrane was incubated with 3% bovine serum albumin in Tris-buffered saline (20 mM Tris, 0.5 M NaCl, pH 7.5; TBS) overnight, and then incubated with 1.0 μg/mL of biotinated AOL lectin in TBST (TBS containing 0.05% Tween 20) for 1 h. After washing with TBST, the membrane was incubated with horseradish peroxidase-conjugated avidin (VECTASTAIN ABC kit, Vector Laboratories, Burlingame, CA) for 1 h and then washed with TBST. Staining was performed with ECL Western blot detection reagents (GE Healthcare U.K. Ltd., Buckinghamshire, England).

Lectin Affinity Electophoresis Using LCA Lectin

Lectin affinity electrophoresis using LCA (*Lens culinaris*) lectin was performed with the AFP-L3 Differentiation Kit L (Wako Pure Chemicals, Osaka, Japan) according to the manufacturer's instructions. Briefly, 2-μL samples were subjected to electrophoresis on an agarose gel containing LCA lectin. The separated AFP was transferred to the membrane attached human AFP antibody by antibody-affinity blotting.

Structural Analysis of Oligosaccharides Derived from Glycoproteins in BC Structures and Medium

Preparations of pyridylamino (PA)-oligosaccharides were performed with BlotGlyco (Sumitomo Bakelite Co., Ltd., Tokyo, Japan) according to the manufacturer's instructions. Structural analyses of PA-oligosaccharides derived from glycoproteins in BC structures and medium were performed by means of the modified method described previously.[14] Briefly, sialic acid moieties on the purified PA-oligosaccharides were removed by neuraminidase treatment (*Arthrobacter ureafaciens*, Nacalai Tesque, Kyoto, Japan) in 0.2 M acetate buffer, pH 7.4, at 37 °C overnight. The asialo PA-

oligosaccharides were separated by reversed-phase high performance liquid chromatography (HPLC) on a Shim-pack CLC-ODS column (Shimadzu Corp., Kyoto, Japan) and subsequent normal phase HPLC on a TSK-gel Amide-80 column (Tosoh Corp., Tokyo, Japan). Elution and detection of PA-oligosaccharides were performed as described by Tomiya et al.[20] The structures of PA-oligosaccharides were determined from the elution positions of individual peaks on the basis of the GALAXY database.[21] The structures of PA-oligosaccharides not registered in the GALAXY database were confirmed by liquid chromatography-electrospray ionization- tandem mass spectrometry (LC-ESI-MS/MS).

Mass Spectrometry

PA-oligosaccharides were analyzed by LC-ESI-MS/MS.[22] HPLC was performed on a Paradigm MS4 equipped with a Magic C18 column (0.2 × 50 mm, Michrome BioResource, Auburn, CA). Each PA-oligosaccharide was injected with a flow rate of 2 μL/min for 3 min and eluted with 50% methanol for 10 min. MS analyses were performed using a LCQ ion trap mass spectrometer (Thermo Finnigan, San Jose, CA) equipped with a nanoelectrospray ion source (AMR, Tokyo, Japan). The nanospray voltage was set at 2.0 kV in the positive ion mode. The heated desolvation capillary temperature was set to 200 °C. In the LCQ method file, the LCQ was set to acquire a full MS scan between 1350 and 2700 m/z followed by MS/MS scans in a data-dependent manner.

RESULTS

Comparison of Oligosaccharide Structures on Glycoproteins Secreted into BC Structures and Medium in HepG2 Cells

We compared the oligosaccharide structures on glycoproteins secreted into BC structures with those on glycoproteins secreted into medium by AOL lectin blot analysis. AOL lectin binds fucose residues.[23] As shown in Figure 1, enhanced intensities of AOL binding were observed in glycoproteins secreted into medium, compared with those in glycoproteins secreted into BC structures. This result was contradictory to the results from previous studies, which showed that many glycoproteins in bile were strongly fucosylated,[13,14] suggesting that the fucosylation-based sorting machinery might be disrupted in HepG2 cells.

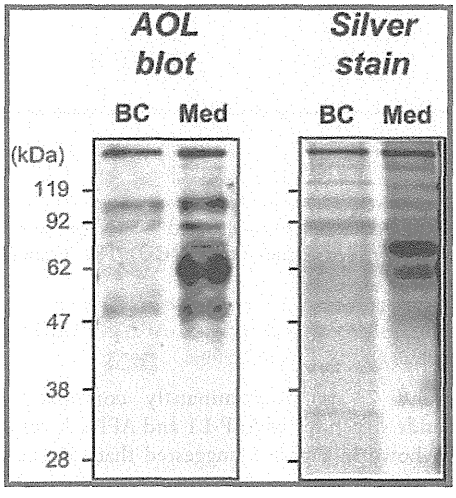

Figure 1. Comparison of the fucosylation levels of glycoproteins secreted into BC structures and into medium. Five micrograms of protein from BC structures and from medium were subjected to silver staining. Lectin blot analysis was performed using the same samples. AOL binds to fucose residues. BC and Med indicate BC structures and medium, respectively. The procedures are described in detail in the Experimental Section.

To determine the oligosaccharide structures on glycoproteins secreted into BC structures and medium in more detail, two-dimensional mapping HPLC and LC-ESI-MS analyses were performed (Table 1). Representative elution profiles of PA-oligosaccharides derived from glycoproteins in BC structures and medium on reversed-phase HPLC are shown in Figure 2. Oligosaccharides specific to BC structures or medium were not observed (Figure 2). As shown in Figure 3, the percentage of peak 7 material on glycoproteins from the medium was larger than that on glycoproteins from BC structures. This result indicated that the enhanced intensities of AOL binding in glycoproteins in the medium might be due to an increase in alpha1−6 fucosylated biantennary structures (peak 7) on glycoproteins.

Determination of the Percentages of Fucosylated AFP Secreted into BC Structures and Medium in HepG2 Cells by LCA-Affinity Electrophoresis

To investigate the polarized secretion of fucosylated AFP in HepG2 cells, the percentages of AFP-L3 in BC structures and medium were determined by LCA-affinity electrophoresis. As shown in Figure 4, the percentage of AFP-L3 in BC structures was higher than that in the medium. This result suggests that fucosylated AFP might be secreted into BC structures preferentially; in other words, AFP might be secreted into BC structures by the sorting machinery via fucosylation.

Suppression of Fucosylation by Double Knock-Down of GMD and FX

As shown in Figure 4, the percentage of fucosylated AFP in medium was also high, although the percentage was smaller than that in BC structures. We previously suggested that the selective secretion of fucosylated glycoproteins into bile might not be disrupted, but might rather be saturated, in the HCC liver in Long-Evans Cinnamon color rats.[14] Therefore, we believed that excess fucosylated glycoproteins, which could not be secreted into BC structures, might be secreted into medium because of the high fucosylation levels in HepG2 cells.

GDP-fucose, a donor substrate for fucosyltransferases, is synthesized via two pathways, the de novo and salvage pathways. The de novo pathway synthesizes GDP-fucose via three reactions catalyzed by GMD and FX, while the salvage pathway synthesizes GDP-fucose from free fucose.[24]

To investigate whether the selective secretion of fucosylated glycoproteins into BC structures is saturated in HepG2 cells, we established cells containing a DKD of GMD and FX. The fucosylation levels in DKD cells should be decreased because of the reduction of GDP-fucose levels. As shown in Figure 5B, fucosylation levels of glycoproteins secreted into the medium in DKD cells were lower than those in wild type. On the other hand, there were no differences between DKD and wild-type cells in the fucosylation levels of glycoproteins secreted into BC structures (Figure 5A).

Next, to rescue the fucosylation levels of glycoproteins in DKD cells, we added 5 mM of free fucose to the medium of DKD cells. The GDP-fucose level is increased via the salvage pathway upon adding free fucose. Increases in fucosylation levels were observed only in glycoproteins secreted into

Table 1. Assignment of the Major PA-Oligosaccharides by Two-Dimensional Mapping HPLC and LC-ESI-MS Analyses

Peak[a]	Structure[b]	ODS[c]	Amide-80[c]	*m/z*[d]
1	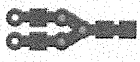	10.3	7.0	1718.9
2	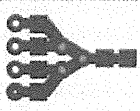	10.3	9.9	2449.5
3	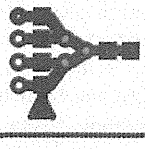	10.3	10.6	2595.2
4	 +▲x2	12.2	8.3	2011.3
5		12.8	8.4	2084.3
6	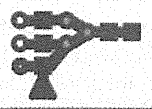	12.8	9.1	2230.2
7	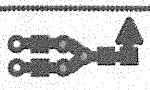	13.5	7.4	1865.4
8	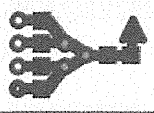	13.5	10.2	2595.2
9	 +▲x3	15.1	9.0	2522.3
10	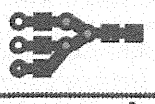 +▲x2	16.6	9.5	2376.3
11	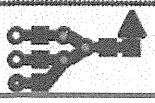	17.0	8.8	2230.2

[a]Numbers at each peak indicated correspond to those in Figures 2, 3, and 6. [b]Monosaccharides were denoted by ○, galactose; ■, *N*-acetylglucosamine; ●, mannose; ▲, fucose. [c]The elution positions on HPLC columns were expressed as glucose units (GU). The chromatographic conditions were described in the Experimental Section. [d]The ions correspond to $[M + H]^+$.

medium upon adding free fucose (Figure 5). Further, we calculated the ratio of peak 7 material to peak 1 material to determine changes in fucosylation level. The percentage of fucosylation in medium was increased upon adding free fucose in DKD cells (Figure 6B). On the other hand, this percentage was almost the same in BC structures in the presence and absence of free fucose in DKD cells (Figure 6A). These results showed that the fucosylated glycoproteins increased in DKD cells upon adding free fucose, and then the glycoproteins were solely secreted into the medium. Taken together, these results suggest that the secretion of fucosylated glycoproteins into BC structures might be saturated in HepG2 cells.

Polarized Secretion of Fucosylated AFP in HepG2 Cells with Different Fucosylation Levels

Peaks 1 and 7 are predominantly composed of the oligosaccharide structures of AFP-L1 and AFP-L3, respectively. The result shown in Figure 6 suggested that the secretion of fucosylated AFP into BC structures might be saturated and that the excess fucosylated AFP might be secreted into medium. To verify this, we compared the percentages of AFP-L3 secreted into BC structures and medium between HepG2 cells with different fucosylation levels by LCA-affinity electrophoresis. As shown in Figure 7B, the percentage of AFP-L3 secreted into medium was decreased in DKD cells, compared with wild-type cells, and an increase in the percentage of AFP-L3 was observed

dx.doi.org/10.1021/pr201154k | *J. Proteome Res.* 2012, 11, 2798–2806

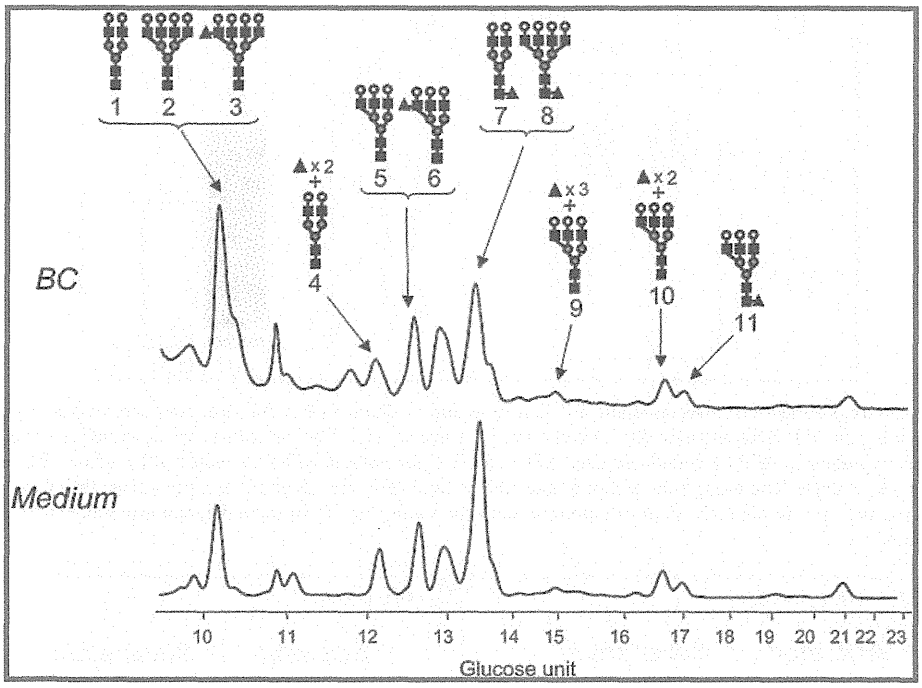

Figure 2. HPLC separation of PA-oligosaccharides derived from glycoproteins in BC structures and medium. Representative elution profiles of PA-oligosaccharides derived from glycoproteins in BC structures (top) and medium (bottom) on an ODS column. The numbers of the peaks and the symbols for monosaccharides correspond to those in Figures 3 and 6 and Table 1. The procedures are described in detail in the Experimental Section.

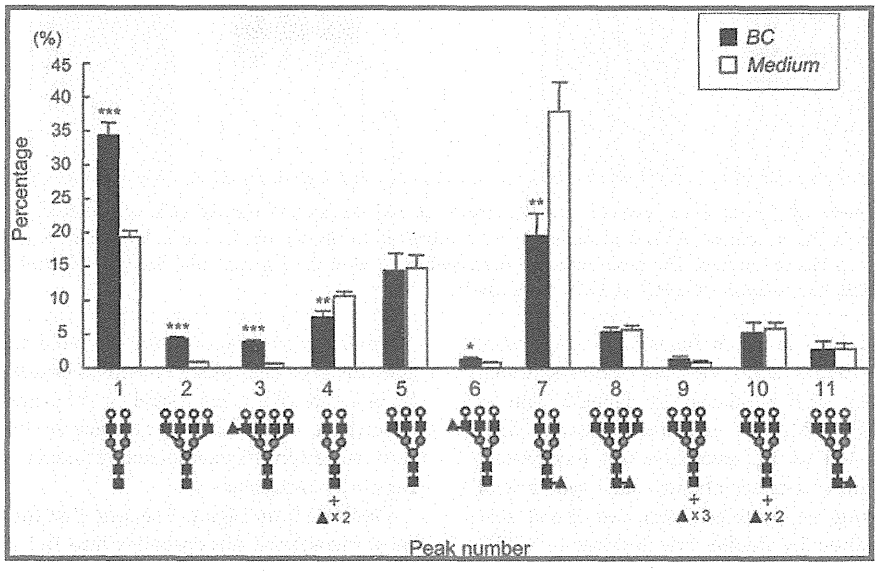

Figure 3. Percentages of oligosaccharide structures on glycoproteins in BC structures and medium. Percentages of each oligosaccharide structure in the total area of the assigned peaks were calculated on the basis of the peak areas from the ODS and Amide-80 elution profiles. The numbers of the peaks and the symbols for monosaccharides correspond to those in Figures 2 and 6 and Table 1. Closed and open columns indicate BC structures and medium, respectively. Each column represents the mean plus SD for three different experiments. *, significantly different ($p < 0.05$) from medium; **, significantly different ($p < 0.01$) from medium; ***, significantly different ($p < 0.001$) from medium.

by adding free fucose in DKD cells. On the other hand, there were no significant differences in the percentages of AFP-L3 secreted into BC structures among these three kinds of cells (Figure 7A).

DISCUSSION

Our previous results suggested that fucosylation is a possible signal for the secretion of glycoproteins into bile in the liver and that the fucosylation-based sorting machinery might be disrupted in hepatocarcinogenesis.[13,14] These findings provide an explanation to the increased level of fucosylated AFP seen in sera of HCC patients. In this study, to investigate the secretion mechanism of fucosylated AFP into bile/serum in detail, we analyzed the selective secretion of fucosylated AFP into BC structures and conditioned medium of HepG2 cells.

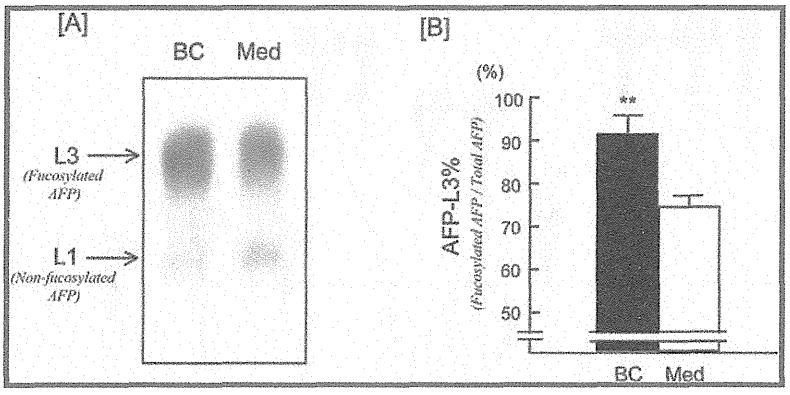

Figure 4. LCA-affinity electrophoresis of AFP secreted into BC structures and medium. AFP in BC structures and medium were subjected to LCA-affinity electrophoresis using an AFP Differentiation Kit L (Wako Pure Chemicals) [A]. The procedures are described in detail in the Experimental Section. The bands corresponding to AFP-L1 (nonfucosylated AFP) and -L3 (fucosylated AFP) are indicated by arrows. BC and Med indicate BC structures and medium, respectively. The proportion of fucosylated AFP in total AFP was calculated as a percentage [B]. Closed and open columns indicate BC structures and medium, respectively. Each column represents the mean plus SD for three different experiments. **, significantly different ($p < 0.01$) from medium.

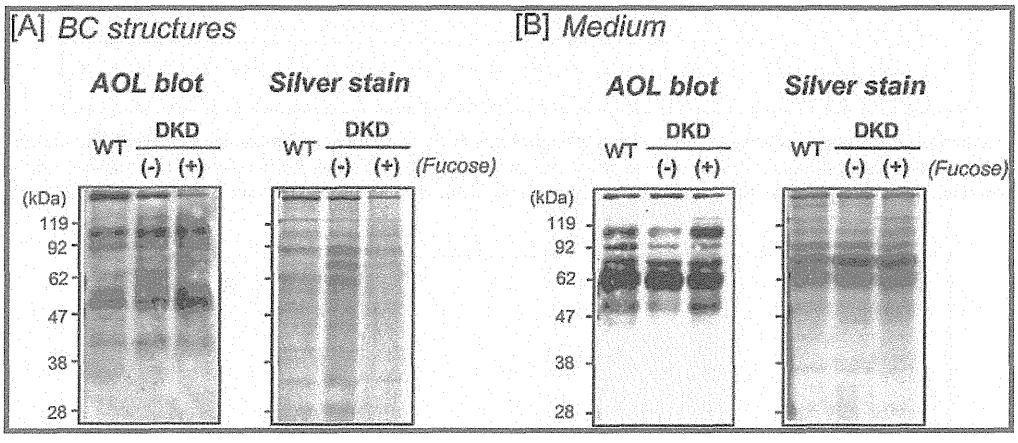

Figure 5. Lectin blot analyses of glycoproteins secreted into BC structures and medium in HepG2 cells with different fucosylation levels. Five micrograms of proteins from BC structures [A] and medium [B] were subjected to silver staining. Lectin blot analyses were performed using the same samples. AOL binds to fucose residues. The procedures are described in detail in the Experimental Section. WT and DKD indicate wild-type cells and cells with a double knock-down of GMD and FX, respectively.

HepG2 cells express high levels of fucosylation regulatory genes, while normal hepatocytes do not express them. Therefore, most of the AFP produced by HepG2 cells is fucosylated AFP (AFP-L3). As expected, greater than approximately 90% of AFP in BC structures was fucosylated, as shown in Figure 4. These data corroborate our hypothesis of fucosylation-based sorting of proteins. Next, we found that suppression of fucosylation by double knock-down of GMD and FX did not reduce the percentage of fucosylated AFP in BC structures, but did decrease the percentage of fucosylated AFP in medium (Figure 7). Furthermore, an increase in fucosylation level was observed in AFP in the conditioned medium, but not in the BC structures, upon adding free fucose (Figure 7). These results suggest that the secretion of fucosylated AFP into BC structures might be saturated in HepG2 cells and that excess fucosylated AFP might be secreted into the medium. This result is consistent with the clinical observation that low levels of AFP-L3 are detected in sera of patients with benign liver disease. More recently, Kuno et al. reported that an increase in fucosylation on serum alpha1-acid glycoprotein (AGP) is associated with liver fibrosis,[25] suggesting that noncancerous hepatocytes with high levels of fucosylation might lead to the saturated secretion of fucosylated proteins into bile. More recently, Hanaoka et al. reported that fucosylated AFP was useful as a prognostic factor for the occurrence of HCC.[26] The results in this study suggest that overexpression of fucosylated proteins is an early event of hepatocarcinogenesis.

Our data from Figure 1 suggest that the selective secretion of most fucosylated glycoproteins into BC structures is disrupted in HepG2 cells. In the absence of such disruption, the fucosylation levels of glycoproteins such as AFP in BC structures should be higher than those in the conditioned medium. It has been reported that an *N*-glycan at a specific site plays a pivotal role in apical sorting in a glycoprotein possessing multiple *N*-glycans.[27] Protein-specific *N*-glycans bearing the responsibility for apical sorting might be involved in selective secretion into bile. Selective secretion via fucosylation of most glycoproteins, with the exception of AFP, might be disrupted in HepG2 cells. Analyses of conformational oligosaccharides on each glycoprotein are required.

We believe that there might be a receptor containing a lectin domain that interacts with fucosylated oligosaccharides and that this receptor could regulate the secretion of soluble

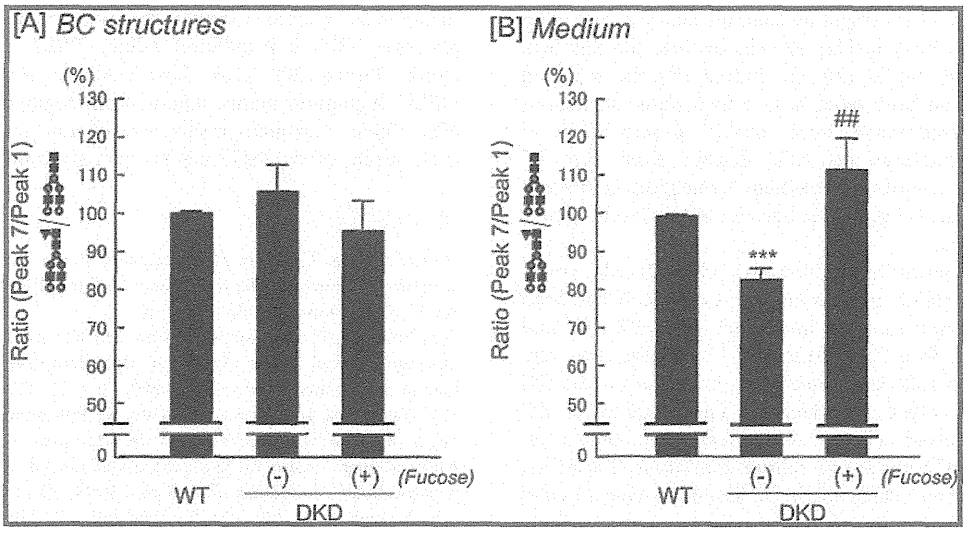

Figure 6. Comparison of the ratio of peak 7 material to peak 1 material between HepG2 cells with different fucosylation levels. The ratio of peak 7 material to peak 1 material from BC structures [A] and medium [B] were calculated on the basis of the peak areas of the ODS and Amide-80 elution profiles, and the values were corrected for that of wild type. The numbers of the peaks and the symbols for monosaccharides correspond to those in Figures 2 and 3 and Table 1. WT and DKD indicate wild-type cells and cells with a double knock-down of GMD and FX, respectively. Each column represents the mean plus SD for three different experiments. ***, significantly different ($p < 0.001$) from wild type; ##, significantly different ($p < 0.01$) from without fucose.

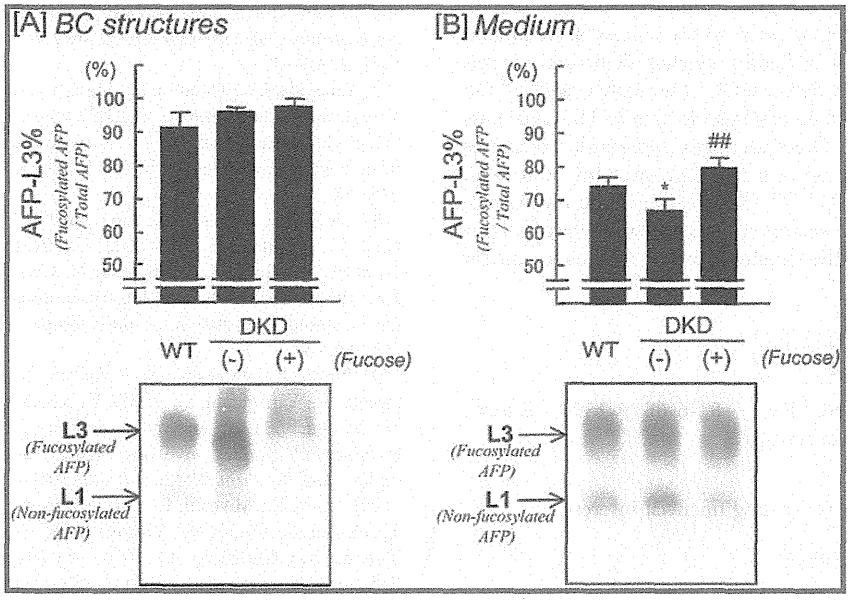

Figure 7. Comparison of the percentages of fucosylated AFP between HepG2 cells with different fucosylation levels. AFP in BC structures [A] and medium [B] from HepG2 cells with three different fucosylation levels were subjected to LCA-affinity electrophoresis using an AFP Differentiation Kit L (Wako Pure Chemicals). The procedures are described in detail in the Experimental Section. The bands corresponding to AFP-L1 (nonfucosylated AFP) and -L3 (fucosylated AFP) are indicated by arrows. WT and DKD indicate wild-type cells and cells with a double knock-down of GMD and FX, respectively. Each column represents the mean plus SD for three different experiments. *, significantly different ($p < 0.05$) from wild type; ##, significantly different ($p < 0.01$) from without fucose.

glycoproteins into bile. Fucosylated AFP might exhibit higher affinity for this receptor and might be given priority for secretion into bile, compared with other glycoproteins such as AGP. Therefore, fucosylated AFP, exhibiting higher affinity for the receptor, might not be secreted into serum in the liver with chronic liver diseases, whereas fucosylated AGP, exhibiting lower affinity, is secreted into serum. Comunale et al. reported that increases in alpha1−6 fucosylation on alpha1-antitrypsin were HCC-specific, while increased outer arm fucosylation was observed in both cirrhosis and HCC patients.[28] This report supports our hypothesis that glycoproteins that possess alpha1−6 fucosylated oligosaccharides, including fucosylated AFP, are more selectively secreted into bile. On the other hand, as shown in Figure 3, a percentage of peak 7 material, alpha1−6 fucosylated biantennary structure, in the conditioned medium was significantly higher than that in the BC structures. These data do not seem to be consistent with our hypothesis that alpha1−6 fucosylated glycoproteins are selectively secreted into